

Autocatalysis in chemical networks: unifications and extensions

Alex Blokhuis,^{1,2} David Lacoste,¹ and Philippe Nghe²

¹⁾*Gulliver Laboratory, UMR CNRS 7083, PSL University, 10 rue Vauquelin, Paris F-75231, France*

²⁾*Laboratoire de Biochimie, Chimie Biologie et Innovation, ESPCI Paris, PSL University, 10 rue Vauquelin, Paris F-75231, France*

(Dated: May 16, 2020)

Autocatalysis is an essential property for theories of abiogenesis and chemical evolution. However, the different formalisms proposed so far seemingly address different forms of autocatalysis and it remains unclear whether all of them have been captured. Furthermore, the lack of unified framework thus far prevents a systematic study of autocatalysis. Here, we derive general stoichiometric conditions for catalysis and autocatalysis in chemical reaction networks from basic principles in chemistry. This allows for a classification of minimal autocatalytic motifs, which includes all known autocatalytic systems and motifs that had not been reported previously. We further examine conditions for kinetic viability of such networks, which depends on the autocatalytic motifs they contain. Finally, we show how this framework extends the range of conceivable autocatalytic systems, by applying our stoichiometric and kinetic analysis to autocatalysis emerging from coupled compartments. The unified approach to autocatalysis presented in this work lays a foundation towards the building of a systems-level theory of chemical evolution.

PACS numbers: 05.40.-a 82.65.+r 82.20.-w

INTRODUCTION

Life’s capacity to make more of itself is rooted in a chemistry that makes more of itself. Autocatalysis appears to be ubiquitous in living systems from molecules to ecosystems¹. It is also likely to have been continually present since the beginning of life and is invoked as a key element in prebiotic scenarios^{2–5}. However, autocatalysis is considered to be a rarity in chemistry⁶. This would suggest that prebiotic molecules may not be that different from biomolecules (lipids^{4,5}, nucleic acids^{7–10}, and peptides^{2,3}).

Developments in systems chemistry are changing this view, with an increasing number of autocatalytic systems synthesized de novo^{11–13}. Chemical replicators have been endowed with biomimetic properties such as protein-like folding¹⁴ and parasitism¹⁵. Autocatalysis also finds technological applications, e.g. enantiomere and acid amplification^{16–18}.

The elucidation of autocatalysis represents a primary challenge for theory. Models based on autocatalysis were first built to explain a diversity of dynamical behaviors in so called dissipative structures, such as bistable reactions¹⁹, oscillating reactions, chemical waves²⁰ and chemical chaos. Autocatalysis then became a central topic for studying the self-replication dynamics of biological and prebiotic systems^{3,21–23} (see^{24–26} for recent reviews).

Despite this long history, a unified theory of autocatalysis is still lacking. Such a theory is needed to understand the origins, diversity and plausibility of autocatalysis. It would also provide design principles for artificial autocatalytic systems.

Here, we present a framework that unifies the

different descriptions of autocatalysis and is based on reaction network stoichiometry^{27–30}.

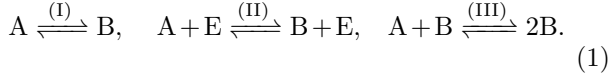
Let us start from basic definitions in chemistry as established by IUPAC³¹ (see Supplementary Information Section I for full definitions), where autocatalysis is a particular form of catalysis: *A substance that increases the rate of a reaction without modifying the overall standard Gibbs energy change (ΔG°) in the reaction; the process is called catalysis. The catalyst is both a reactant and product of the reaction. Catalysis brought about by one of the products of a (net) reaction is called autocatalysis.*

From this definition, we derive conditions to determine whether a subnetwork embedded in a larger chemical network, can be catalytic or autocatalytic. These conditions provide a mathematical basis to identify minimal motifs, called autocatalytic cores. Cores come in five structural motifs. They allow classification of all previously described forms of autocatalysis, and also reveal not yet identified autocatalytic schemes. We then study the kinetic conditions, which we call viability conditions, under which autocatalytic networks can appear and be maintained on long times. We find that networks have a different viability depending on their core structure, notably that internal catalytic cycles increase robustness. Finally, we expand the repertoire of autocatalytic systems, by demonstrating a general mechanism for its emergence on a multicompartment level. This mechanism strongly relaxes chemical requirements for autocatalysis, making the phenomenon more abundant and diverse than previously thought.

EXAMPLES, DEFINITIONS AND CONVENTIONS

Catalysis and autocatalysis

The following reactions have the same net mass balance but a different status regarding catalysis:



Since no species is both a reactant and product in reaction (I), it should be regarded as uncatalyzed. Reactions (II) and (III) instead contain species which are both a reactant and a product, species E in reaction (II) and species B in reaction (III) and following the definition above, these species can be considered as catalysts. In reaction (II), the amount of species E remains unchanged, in contrast to the case of reaction (III), where the species B experiences a net production. For this reason, reaction (III) represents genuine autocatalysis. Although reaction (II) is usually referred to as simply catalyzed in the chemistry literature, we propose to call it an example of allocatalysis to contrast it with the case of autocatalysis. Then, we can reserve the word catalysis for any instance and combination of allocatalysis, autocatalysis and reverse autocatalysis.

We emphasize that such stoichiometric considerations are necessary but not sufficient to characterize catalysis, which according to the definition should also accelerate the rate of the net reaction. In the following, we will first generalize the stoichiometric conditions, then examine kinetic ones.

Stoichiometric matrix and reaction vectors

Reaction networks are represented as a stoichiometric matrix $\nu^{27,30}$, in which columns correspond to reactions and rows to species. The entries in a column are the stoichiometric coefficients of the species participating in that reaction, the coefficient is negative for every species consumed and positive for every species produced. A reaction vector $\mathbf{g} = [g_1, \dots, g_r]^T$ results in a change of species numbers $\Delta \mathbf{n} = \nu \cdot \mathbf{g}$. The support of \mathbf{g} (denoted $\text{supp}(\mathbf{g})$) is the set of its non-zero coordinates. A reaction cycle is a non-zero reaction vector \mathbf{c} such that no net species number change occurs: $\nu \cdot \mathbf{c} = \mathbf{0}$, or equivalently, \mathbf{c} belongs to the right null space of ν . Vectors \mathbf{b}^T belonging to the left null space of ν induce conservation laws, because in that case $\mathbf{b} \cdot \mathbf{n}$ represents a conserved quantity. The case of all coefficients b_k nonnegative is referred to as a mass-like conservation law. For example in Fig.1a, conserved quantities are $n_E + n_{EA}$ (catalysts) and $n_A + n_{EA} + n_B$ (total compounds).

Lastly, catalyzed reactions may not always be distinguished from uncatalyzed one in the stoichiometric

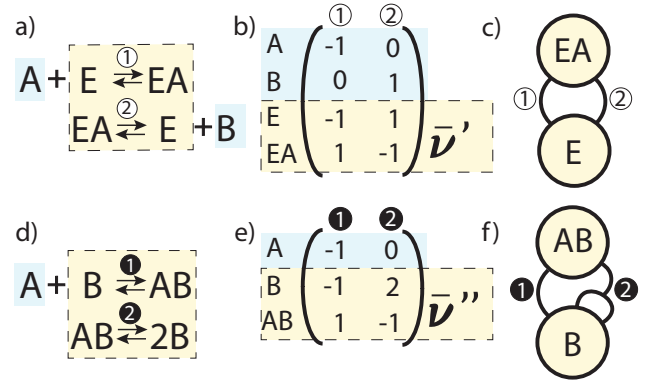
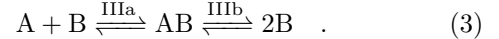
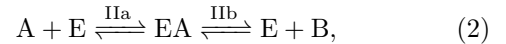


Figure 1: Different representation for allocatalysis (a,b,c) and autocatalysis (d,e,f). a) Combining reactions (1')+(2') affords an allocatalytic cycle that converts A to B. b) stoichiometric matrix of a), the dashed square encloses the allocatalytic submatrix ν' for network b). c) Graph representation of the allocatalytic subnetwork. d) Combining (1'')+(2'') affords an autocatalytic cycle converting A to B. e) stoichiometric matrix of d), the dashed square encloses the autocatalytic submatrix ν'' for network e). f) a graph representation of the autocatalytic subnetwork.

matrix. For instance, in reactions (II-III), catalysts cancel on each side leading to the same column vector as for (I). One way to avoid this is to describe enough intermediate steps so that a participating species is either a reactant or a product:



We call this convention non-ambiguity and assume henceforth that it is respected.

CATALYSIS AND AUTOCATALYSIS IN STOICHIOMETRIC MATRICES

We seek to identify candidate motifs (subnetworks) for allocatalysis and autocatalysis within reaction networks based on the only knowledge of the stoichiometric matrix ν . Such identification does not make a priori assumptions on the values or signs of reaction vector coefficients, or on kinetics, which we will examine in the next section. A motif has a stoichiometric submatrix $\bar{\nu}$ obtained by restricting ν to certain rows and columns.

Restriction to rows delimitates species within the system from external species³⁰, such as feedstock compounds (also so-called food set³²) and waste. In Fig. 1, external species have been colored in blue, while stoichiometric submatrices have been boxed in yellow. Fig. 1a (resp. Fig. 1d) represents an example of allocatalysis (resp. autocatalysis) with its submatrix ν' (resp. ν'') and its hypergraph representation Fig. 1c (resp. Fig.

1f).

We restrict further the stoichiometric matrix to some reactions (columns). We do that in order to guarantee that each reaction of the subsystem has at least one reactant and at least one product. The subsystem then has a property called autonomy, which means that every column of the reduced matrix contains a positive and a negative coefficient²⁸. Autonomy ensures that the production any catalyst is conditional on the presence of other chemical species of the subsystem (similarly to the siphon concept in Petri Nets³³ but without assumption on reaction signs, see Supplementary Information Sections II and III). Otherwise, rate acceleration would be allowed unconditional on an already present substance, in opposition to the definition of catalysis.

Criterion for allocatalysis

By definition, allocatalysis is an ensemble of reactions by which a set of species remain conserved in number (the catalysts) while other external species undergo a turnover which changes their numbers. This leads to the following conditions:

There exists a set of species \mathbf{S} , a submatrix $\bar{\nu}$ of ν restricted to \mathbf{S} , and a non-zero reaction vector \mathbf{c} such that: i) $\bar{\nu}$ is autonomous; ii) $\text{supp}(\mathbf{c})$ is included in the columns of $\bar{\nu}$; iii) \mathbf{c} is a reaction cycle of $\bar{\nu}$ ($\bar{\nu} \cdot \mathbf{c} = \mathbf{0}$), and; iv) $\nu \cdot \mathbf{c} \neq 0$. The members of \mathbf{S} which participate to \mathbf{c} (i.e. that are consumed and produced) are called allocatalysts, \mathbf{c} an allocatalytic cycle and $\bar{\nu}$ an allocatalytic matrix.

Condition (i) has been discussed above. Condition (ii) expresses the involvement of the catalysts in the reactions \mathbf{c} , where all columns of $\bar{\nu}$ are non-zero due to (i), so that all reactions of \mathbf{c} involve catalysts. Condition (iii) expresses the conservation of catalysts and (iv) the net reaction. Since the reaction cycle \mathbf{c} is a cycle of the reduced matrix but not of the original matrix, some authors have called it emergent³⁰. This emergent cycle can establish a non-equilibrium steady state driven by the turnover of the external species. Note that being allocatalytic is not a property of the sub-matrix $\bar{\nu}$ alone but requires to explicit its relationship with the larger matrix ν as imposed by condition (iv). A counterexample would be an isomerization cycle, which verifies conditions (i-iii) but is not allocatalytic.

Criterion for autocatalysis

By definition, autocatalysis is the process by which a combination of reactions involves a set of species which all increase in number conditionally on species in the set itself (the autocatalysts). This leads to the following conditions:

There exists a set of species \mathbf{S} , a submatrix $\bar{\nu}$ of ν restricted to \mathbf{S} , and a reaction vector \mathbf{g} such that: i) $\bar{\nu}$ is autonomous, ii) all coordinates of $\Delta \mathbf{n} = \bar{\nu} \cdot \mathbf{g}$ are strictly positive, or equivalently, $\bar{\nu}$ has no mass-like conservation laws. The members of \mathbf{S} consumed (and produced) by \mathbf{g} are called autocatalysts, \mathbf{g} an autocatalytic mode and $\bar{\nu}$ an autocatalytic matrix.

Condition (i) ensures the conditionality of the reactions on autocatalysts, as it forbids cases where species of \mathbf{S} are produced from external reactants only, thus playing the role of conditions (i) and (ii) in the definition of allocatalysis.

Condition (ii) expresses the increase in autocatalysts number. The equivalence between its two formulations is an immediate consequence of Gordan's theorem³⁴. Importantly, the second formulation of (ii) does not involve an autocatalytic mode \mathbf{g} , so that (i) and (ii) can be formulated as properties of a matrix itself, in contrast with allocatalysis. This allows us to look for minimal autocatalytic motifs, which we do next. Note that there is no need to specify an explicit condition on the turnover of external species (as condition (iv) does for allocatalysis), their consumption being implied by the net mass increase imposed by condition (ii).

Autocatalytic cores

An autocatalytic core is an autocatalytic motif which is minimal in the sense that it does not contain any smaller autocatalytic motif. Consequently, an autocatalytic system is either a core, or it contains one or several cores. The stoichiometric conditions show that characterizing cores is equivalent to finding all autonomous matrices whose image contains vectors with strictly positive coordinates only. This well-posed formulation allowed us to show that the stoichiometric matrix $\bar{\nu}$ of an autocatalytic core must verify the specific properties below (see Supplementary Information Sections II - IV for demonstrations and examples).

First, $\bar{\nu}$ must be square (the number of species equals the number of reactions) and invertible. The inverse has a chemical interpretation. By definition of the inverse, the k -th column of $\bar{\nu}^{-1}$ is a reaction vector such that species k increases by one unit, making it an elementary mode of production. Likewise, the reaction vector obtained by summing the columns of $\bar{\nu}^{-1}$ leads to increase by one unit of every autocatalyst, and thus is an elementary mode of autocatalysis. This shows how stoichiometry informs on fundamental modes of autocatalysis³⁵.

Second, every forward reaction of a core involves only one core species as a reactant. While this excludes reactions between two different core species, a single core species may react with itself. As $\bar{\nu}$ is square, this also implies that every species of a core is con-

sumed (none is only produced), thus is an autocatalyst. Furthermore, every species is the reactant of a single reaction. Overall, every species is uniquely associated with a reaction as being its reactant, so that $\bar{\nu}$ admits a representation with a negative diagonal and zero or positive coefficients elsewhere, at least one coefficient of each column being strictly positive to ensure autonomy.

These properties are constraining enough to allow an exhaustive enumeration of reaction graphs that are cores. Autocatalytic cores are found to belong to five categories, denoted as type I to type V. Fig. 2a represents typical members of each category as reaction hypergraphs (see Supp. Fig. S1 for general cases). As can be seen in these graphs, all minimal motifs contain a fork, which ends either in the same compound (or node) for type I or in different compounds for types II to V. This fork is consistent with the intuition that autocatalysis requires reaction steps that amplify the amount of autocatalysts. The orange square on the links between the nodes indicate that these links could contain further nodes and reactions in series.

The five types differ in their number of graph cycles³⁶ and the way these cycles overlap. Type I consists of a single graph cycle that is asymmetric in a stoichiometric sense: the product of the stoichiometric coefficients of its reaction products must be larger than that its reactants. Types II-V can be described as two overlapping graph cycles, where any graph cycle that does not contain all core species must be an allocatalytic cycle (it would otherwise be of Type I, contradicting minimality). Equivalently, the product of the stoichiometric coefficients of the reaction products of these cycles must be equal to that of their reactants.

Unification: First Examples

The stoichiometric characterization of autocatalysis provides a unified approach to autocatalytic networks reported in the literature. The examples below and their proofs are detailed in Supplementary Information Section IV. The formose reaction is a classical example of autocatalysis known to contain many autocatalytic cycles³⁸. Fig. 2b and c show Type I and II cores both found in the formose reaction. Similarly, autocatalytic cores of Type I and II can be found in the Calvin cycle and reverse Krebs cycle (Sup. Fig. S4a). Some reaction steps Fig. 2b may be catalyzed externally (e.g. by enzymes, base, ions), but external catalysis in general does not alter the core. By the same token, proposed examples of auto-induction^{25,39} are found to harbor Type I and II cores (Sup. Fig. S4b).

In the GARD model for self-enhancing growth of amphiphile assemblies^{4,5}, all underlying autocatalysis is described (Supp. Fig. S6) by Type I cycles⁴⁰ (self-incorporation) and Type II cycles built up from

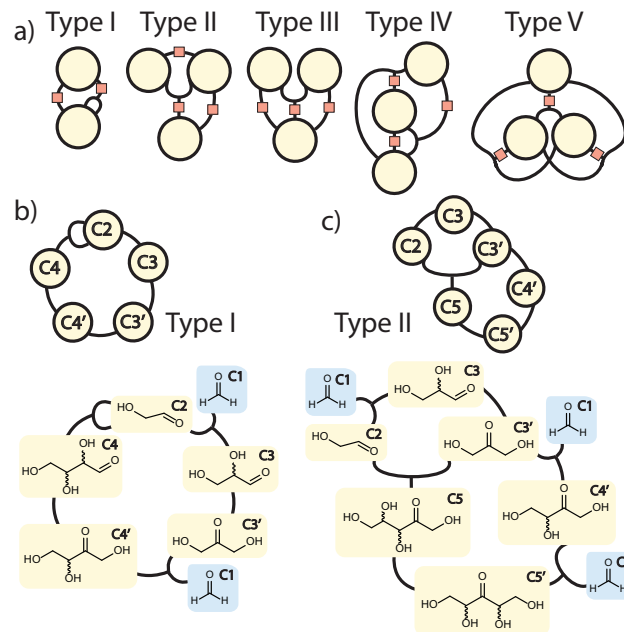


Figure 2: a. Five minimal motifs. Orange squares indicate where further nodes and reactions may be added, provided this preserves the motif type (I,II,III,IV,V) and minimality. b+c: Examples of chemical networks, along with their autocatalytic cores. blue: external species, yellow: autocatalysts. b. Type I: Breslow's 1959 mechanism for the formose reaction³⁷ c. Type II: Another autocatalytic cycle in the formose reaction. Species denoted as Cx inside the nodes refer to molecules containing x carbon atoms, which are shown below in standard chemical representation.

sequential nonoverlapping allocatalytic cycles (cross-incorporation, such as N_3 in Fig. (3)). More generally, when such catalytic cycles are compactly written as single reactions (Eq.(1)), they can be treated in the RAF framework³², where they form irreducible RAF-sets⁴¹. This formally establishes the recently suggested link^{5,42} between these models.

Another proposed extension of autocatalysis is 'chemical amplification' due to cavitands⁴³. The mechanism involves a reactive compound in a molecular cage, whose free counterpart can react to form two species that exchange with the caged species, thus amplifying its release. We find that this process can be described within our framework and corresponds to a Type III core (Supp. Fig. S5).

Overall, examples of Types I and II seem most common, whereas have not yet found examples of Types IV and V.

VIABILITY OF AUTOCATALYTIC NETWORKS

Stoichiometric conditions do not guarantee that autocatalytic motifs amplify. Whether an initial auto-

catalyst amplifies or degrades depends on kinetic considerations. To address this 'fixation problem',^{21,26} we examined the probability P_{ex} of extinction (or $1 - P_{ex}$ of fixation) of species within autocatalytic motifs, as a function of transition probabilities of reaction steps.

Considering an homogeneous system with a steady supply of reactants, several authors have noted that in the highly dilute autocatalyst regime, appreciable rates require first-order autocatalysis^{21,26,44}, i.e. each forward reaction step only involves one autocatalyst. Among first-order order networks, fixation models have so far focused on Type I networks (e.g. Fig.2b), which comprise a single graph cycle containing n species. In a transition step, a given species may either proceed irreversibly to the next species or disappear as a result of degradation. King found that if every reaction step k among n steps of the cycle has a success probability Π_k^+ ($1 - \Pi_k^+$ being the degradation probability), fixation is possible if $p_c = \prod_{k=1}^n \Pi_k^+ \geq 1/2$ ⁴⁴, a condition called decay threshold^{23,45}. Bagley et al.²¹ used birth-death processes to derive P_{ex} for an autocatalytic loop comprising one species ($n = 1$). Schuster reported detailed time-dependent statistics for such networks in various contexts²⁶.

Here we extend the problem considered by Bagley et al. so as to include reversible reactions and networks beyond type I using the theory of branching processes⁴⁶. In these stochastic processes, a parent (here an autocatalytic species X_s) is replaced by k offspring, with k drawn from a distribution \mathfrak{P}_k , chemically corresponding to



A procedure to construct the branching process from reaction networks and derive \mathfrak{P}_k from transition probabilities Π_k is illustrated in Supplementary Information Section V. P_{ex} ultimately determines \mathfrak{P}_k , since the probability to go extinct is the probability that all descendants go extinct:

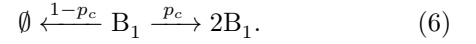
$$P_{ex} = \mathfrak{P}_0 + \mathfrak{P}_1 P_{ex} + \mathfrak{P}_2 P_{ex}^2 + \dots = \sum_{k=0}^{\infty} \mathfrak{P}_k P_{ex}^k. \quad (5)$$

We first exemplify the method by generalizing known results for Type I networks, solutions for other networks are reported in the Supplementary Information Section V. We then compare the computed P_{ex} of autocatalytic motifs which differ in their core structures.

Reversible Type I cycles

Consider a Type I cycle, such as N_1 in Fig. 3b, consisting of n nodes. Starting at the first node, B_1 , let $\mathfrak{P}_2 = p_c$ be the total probability that, after realizing every step of the cycle, it is converted to $2B_1$ ($k =$

2 descendants), and $\mathfrak{P}_0 = 1 - p_c$ the probability of premature degradation:



For reversible reactions, p_c results from the integration of all possible sequences of forward and backward reactions along the cycle. From B_k , let Π_k^- be the transition probability to revert to B_{k-1} , and Π_k^+ to convert to B_{k+1} . We have

$$p_c = \prod_{k=1}^n \Pi_k^+ \Gamma_k, \quad (7)$$

$$\Gamma_{k+1} = \sum_{s=0}^{\infty} (\Pi_{k+1}^- \Gamma_k \Pi_k^+)^s = \frac{1}{1 - \Pi_{k+1}^- \Gamma_k \Pi_k^+}, \quad (8)$$

where Γ_k recursively defines the statistical weight of all back-and-forth trajectories from B_k to itself from the transition probabilities Π_k^- and Π_k^+ , with $\Gamma_1 = 1$. The overall outcome described by (6) corresponds to the simplest type of branching process: a birth-death process. Using (5) finally yields

$$P_{ex} = \begin{cases} \frac{1}{p_c} - 1, & p_c \geq \frac{1}{2}, \\ 1, & p_c < \frac{1}{2}. \end{cases} \quad (9)$$

This generalizes Bagley et al's observation for type I networks to $n > 1$ and reversible reactions. The irreversible limit $\Pi_k^- \rightarrow 0, \Gamma_k \rightarrow 1$ recovers King's result⁴⁴.

Viability of autocatalytic motifs

To investigate how autocatalytic motif structure affects survival, we calculated P_{ex} for five different cores⁴⁷ (N_1 to N_5 , Fig. 3): they are of equal size (6 reaction steps, 6 species), all reactions proceed irreversibly with the same success rate ζ , which plays a similar role as the transition probability Π_k^+ in the example above and is sometimes called specificity^{23,44,45}.

Fig. 3c highlights how P_{ex} depends on ζ for each core structure. The highest ζ for extinction ($P_{ex} = 1$) is observed for the Type I cycle N_1 , and progressively lower values are found for N_2 to N_4 , which are all of type II. Type V network N_5 tolerates the lowest specificity ζ before extinction, sustaining almost three times higher failure rates $1 - \zeta$ than N_1 . These differences can be qualitatively understood by counting the minimum number of steps needed to produce more autocatalysts. In respective order, networks N_1 to N_5 in Fig. 3b do so in six, four, three, three and two steps. In particular, given their symmetries, the P_{ex} of N_3 and N_5 have the same dependence on ζ as a 3 and 2-membered Type I cycle, respectively.

It has been suggested that large networks are dis-

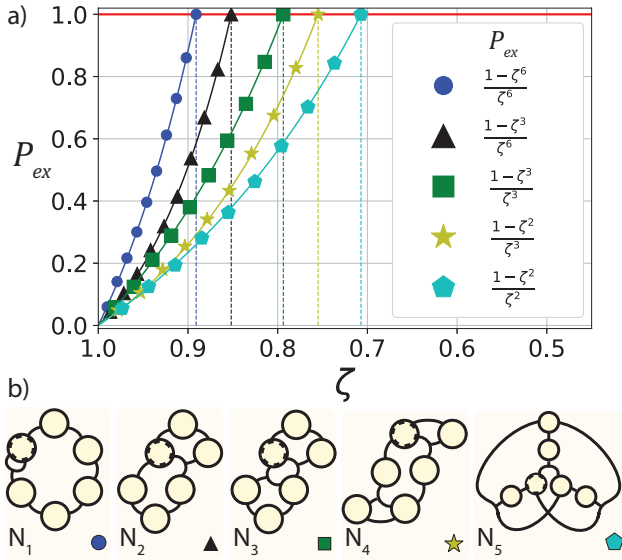


Figure 3: a) P_{ex} as function of ζ (legend: $P_{ex}(\zeta)$ for $P_{ex} < 1$) for b) 5 autocatalytic networks of similar size, starting at the dashed node. N_1 : Type-I cycle. N_2 : Type-II with one fork. N_3 : Type-II, two nonoverlapping allocatalytic cycles, a common motif in GARD with a 1st order RAF representation. N_4 : Type-II: allocatalytic cycles connected by intermediate steps. N_5 : Type-V d) Symbols: P_{ex} after 1000 simulated trials, lines: exact solution. Full expressions are derived in Supplementary Information Section VI.

424 favored in general. The examples of Fig. 3 indicate
 425 that this can be counterbalanced by the presence of
 426 more allocatalytic cycles in the network. In particular,
 427 autocatalytic sets in the sense of RAF-sets allow to
 428 build large and robust networks, since their underlying
 429 structure is typically built up from allocatalytic cycles.

EXTENSION TO MULTICOMPARTMENT AUTOCATALYSIS

430 As a final illustration, we now extend our stoichio-
 431 metric method to an emergent type of autocatalysis.
 432 Consider two compartments α and β , the internal chem-
 433 istry of which admits no autocatalysis (Fig. 4). The
 434 two compartments allow the same chemistry, but they
 435 do not have the same access to feedstock species (U, V
 436 in α and A in β). Upon coupling these compartments
 437 via a membrane that exchanges A and A_2B (Fig. 4a),
 438 a Type II autocatalytic core emerges (Fig. 4b).

441 Here, species AB is limiting in α , whereas in β it is
 442 an abundant feedstock, which is catalytically exchanged
 443 through the reversible formation of A_2B . By coupling
 444 compartments, compounds are no longer restricted to
 445 one role (e.g. feedstock, autocatalyst) and chemical
 446 reactions are no longer restricted to one direction. The
 447 reaction used for reproduction in α is then allowed

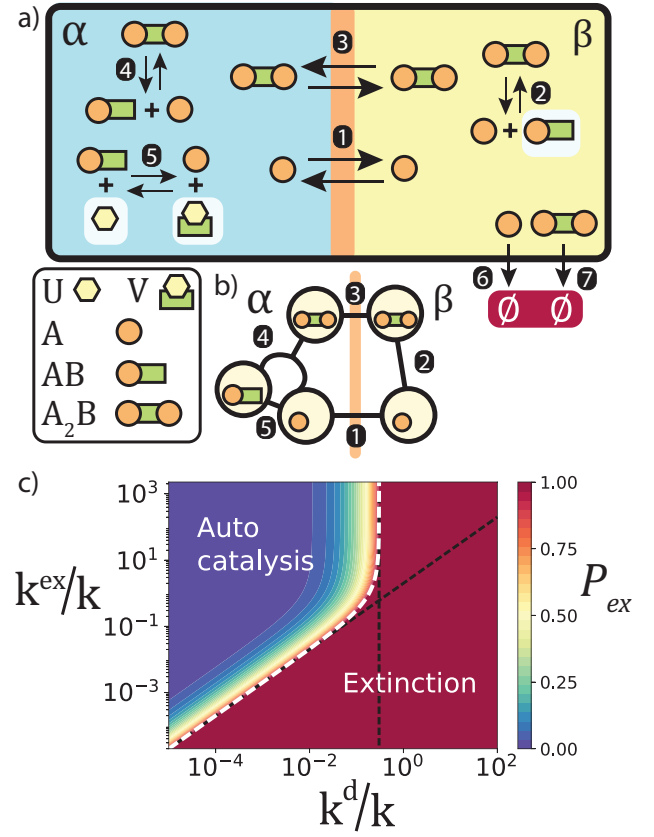


Figure 4: Multicompartment autocatalysis a) between compartments α and β , coupled by exchange reactions of species A and A_2B . AB functions as an autocatalyst in α , and as a feedstock species in β . b) Type III autocatalytic core obtained for the multicompartment autocatalytic network c) Extinction probability P_{ex} for multicompartment autocatalysis in a), starting from a single A_α , as a function of exchange rate k^{ex} and degradation rate k^d , relative to other relevant reaction rates fixed at k (P_{ex} is independent of rates for r_1 and r_5). Sloped asymptote: exchange-limited survival $k_{ex} = 2k^d$. Vertical asymptote: reaction-limited survival $k^d/k = \frac{\sqrt{13}-3}{2}$. The transition between extinction and potential survival ($P_{ex} < 1$) is marked by a dashed white line (solutions for P_{ex} and asymptotes are derived in Supplementary Information Section VIII).

448 to be reused in β , thereby providing the missing loop
 449 to close the cycle. With three compartments, a type
 450 III motif can be constructed from a single bimolecular
 451 reaction (Supp. Fig. S9e).

452 In Fig. 4c, the results of the analysis of the viabil-
 453 ity conditions for this network are shown as a plot of
 454 the extinction probability vs. degradation rate k^d , and
 455 exchange rate k^{ex} . Both of these rates are normalized
 456 by characteristic rates k present in the other reactions
 457 which are assumed to be equal to each other.

458 The figure shows that to overcome the degrada-
 459 tion threshold ($P_{ex} < 1$), the typical reaction rate k

over a certain fraction of the degradation rate k^d (vertical black dotted line in Fig. 4c), as we have seen in the case of single compartment autocatalysis, but additionally, the rate of exchange k^{ex} must outpace the rate of degradation (black oblique dotted line in Fig. 4c). Stochastic simulations (Supp. Fig. S9c) show autocatalytic growth in these conditions for surviving populations, thus confirming that these emergent motifs can indeed exhibit to autocatalysis.

DISCUSSION

We presented a theoretical framework for autocatalysis based on stoichiometry, which allows a precise identification of the different forms of autocatalysis. Starting with a large stoichiometric matrix, we show how to reduce it, and how to distinguish allocatalysis from autocatalysis at the level of this reduced stoichiometric matrix. A detailed analysis of the graph structure contained in these reduced stoichiometric matrices reveals that they contain only five possible recurrent motifs, which are minimal in the sense that they do not contain smaller motifs. Fundamental modes of production of minimal autocatalytic cores are encoded in the column vectors of the inverse of the autocatalytic core submatrix. Autocatalytic cores are found to have a single reactant for each reaction. This means that autocatalytic networks require the availability of certain chemical species in their cores to operate properly. Conversely, the same property also implies that the proper functioning of an autocatalytic network will guarantee the stable supply of certain products, a definitive advantage when these products are key enzymes or metabolites.

We identified these minimal motifs in known examples of autocatalysis such as the formose reaction, metabolic networks, the GARD model and RAF sets. Autocatalytic cores also provide a basis for algorithms to identify these recurring autocatalytic motifs in large chemical networks^{48,49}, as has been done for gene regulatory networks⁵⁰. In this way, we may be able to break the complexity of large chemical networks into smaller, more manageable structures.

Autocatalytic motifs are found to confer different degrees of robustness, which we evaluated using the notion of viability. This viability can be precisely evaluated as a survival probability in an appropriately defined branching process. This approach is applicable to many models for autocatalytic systems upon identification of their cores, highlighting the interest of a unified framework. Viability results from a competition between reactions that produce autocatalysts and side-reactions such as degradation. This is intimately related to the 'paradox of specificity': autocatalytic motifs are more likely to be found in large networks with many different chemical components engaging in many

different reactions. However, putting all those components together disproportionately favors side-reactions, leading to extinction^{23,45}.

Multicompartment autocatalysis introduced here offers a way around this problem: coupled compartments can produce autocatalysis from few reactions and generate extensive networks without mixing all components, thereby reducing the accumulation of degradative side reactions. Overcoming degradation is a general issue, known as the error threshold when replicators degrade by mutation. Compartments also relax this threshold⁵¹, particularly when they are transient⁵².

The emergence of multicompartment autocatalytic cycles relies on the environmental coupling of reaction networks, which allows to access conditions unattainable in a single compartment. In our example, this allowed us to reuse the compounds and reactions to complete autocatalytic cycles. The principle is more general, however: autocatalysis may come from pairing physico-chemical conditions which cannot coexist in one homogeneous phase, as found in the autocatalytic dissolution of copper⁵³ and pitting corrosion. Such principles may be exploited to more readily design autocatalytic systems with biomimetic functionalities.

Overall, our framework shows that autocatalysis comes in a diversity of forms and can readily emerge in unexpected ways, which makes autocatalysis in chemistry more widespread than previously thought. This invites to search for further extensions of autocatalysis, which provides new vistas⁵⁴ for understanding how chemistry may complexify towards life.

MATERIALS AND METHODS

Theoretical methods and derivation of results are detailed in the Supplementary Information, which is divided up in the following sections: I) Terminology and definitions, II) derivation of autocatalytic cores from Graph theory, III) their chemical interpretation and IV) application to formose, autoinduction, metabolic cycles, chemical amplification, RAF sets, GARD V) branching process derivation and determination of P_{ex} . VI) determination of P_{ex} for Fig. 3. VII) determination of P_{ex} for Fig. 4d. VIII) autocatalysis from one bimolecular reaction and 3 compartments.

ACKNOWLEDGEMENTS

AB acknowledges stimulating discussions with D. van de Weem. AB and DL acknowledge support from Agence Nationale de la Recherche (ANR-10-IDEX-0001-02, IRIS OCAV). PN acknowledges C. Flamm for discussions.

REFERENCES

- ¹W. Hordijk, *BioScience* **63**, 877 (2013).
- ²A. I. Oparin, *Origin of Life* (Dover, 1952).
- ³S. A. Kauffman, *J. Theor. Biol.* **119**, 1 (1986).
- ⁴D. Segré, D. Ben-eli, D. W. Deamer, and D. Lancet, *Orig. Life Evol. Biosph.* **31**, 119 (2001).
- ⁵D. Lancet, R. Zidovetzki, and O. Markovitch, *J. R. Soc. Interface* **15**, 20180159 (2018).
- ⁶L. E. Orgel, *Plos Biol.* **6**, 5 (2008).
- ⁷C. Woese, *The Genetic Code, the Molecular Basis for Genetic Expression* (Harper and Row, New York, 1967).
- ⁸L. E. Orgel, *J. Mol. Biol.* **38**, 381 (1968).
- ⁹F. Crick, *J. Mol. Biol.* **38**, 367 (1968).
- ¹⁰W. Gilbert, *Nature* **319**, 618 (1986).
- ¹¹A. Bissette, B. Odell, and S. Fletcher, *Nat Commun* **5**, 4607 (2014).
- ¹²S. N. Semenov, L. J. Kraft, A. Ainla, M. Zhao, M. Baghbazadeh, V. E. Campbell, K. Kang, J. M. Fox, and G. M. Whitesides, *Nature* **537**, 656 (2016).
- ¹³H. N. Miras, C. Mathis, W. Xuan, D.-L. Long, R. Pow, and L. Cronin, *Proc. Natl. Acad. Sci. U. S. A.* (2020), 10.1073/pnas.1921536117.
- ¹⁴B. Liu, C. G. Pappas, E. Zangrando, N. Demitri, P. J. Chmielewski, and S. Otto, *J. Am. Chem. Soc.* **141**, 1685 (2019).
- ¹⁵M. Altay, Y. Altay, and S. Otto, *Angew. Chem. Int. Ed.* **57**, 10564 (2018).
- ¹⁶C. Viedma, *Phys. Rev. Lett.* **94**, 065504 (2005).
- ¹⁷I. Baglai, M. Leeman, M. Kellogg, and W. Noorduyn, *Org. Biomol. Chem.* **17**, 35 (2019).
- ¹⁸K. Ichimura, K. Arimitsu, and K. Kudo, *Chemistry Lett.* **24**, 551 (1995).
- ¹⁹F. Schlögl, *Z. Phys.* **253**, 147 (1972).
- ²⁰G. Nicolis and I. Prigogine, *Self-Organization in Nonequilibrium Systems: From Dissipative Structures to Order through Fluctuations* (Wiley, New York, 1977).
- ²¹R. J. Bagley, D. J. Farmer, and W. Fontana, in *Artif. Life II* (1991) pp. 141–158.
- ²²D. Segré, D. Lancet, O. Kedem, and Y. Pilpel, *Orig. Life Evol. Biosph.* **28**, 501 (1998).
- ²³E. Szathmáry, *Philos. Trans. R. Soc. Lond. B. Biol. Sci.* **361**, 1761 (2006).
- ²⁴W. Hordijk and M. Steel, *Journal of Theoretical Biology* **227**, 451 (2004).
- ²⁵D. G. Blackmond, *Angew. Chem. Int. Ed.* **48**, 386 (2009).
- ²⁶P. Schuster, *Monatsh. Chem.* **150**, 763 (2019).
- ²⁷M. Feinberg, *Foundations of Chemical Reaction Network Theory* (Springer, New York, 2019).
- ²⁸U. Barenholz, D. Davidi, E. Reznik, Y. Bar-on, N. Antonovsky, E. Noor, and R. Milo, *eLife* **6**, e20667 (2017).
- ²⁹A. Deshpande, M. Gopalkrishnan, and C. Science, *Bull. Math. Biol.* **76**, 2570 (2014).
- ³⁰M. Polettini and M. Esposito, *J. Chem. Phys.* **141**, 024117 (2014).
- ³¹A. D. McNaught and A. Wilkinson, *IUPAC Compendium of Chemical Terminology, 2nd ed. ("the Gold Book")* (Blackwell Scientific Publications, Oxford, 1997).
- ³²W. Hordijk, *J. Theor. Biol.* **435**, 22 (2017).
- ³³M. Gopalkrishnan, *Bull. Math. Biol.* **73**, 2962 (2011).
- ³⁴Borwein, Jonathan and Lewis, Adrian S., *Convex Analysis and Nonlinear Optimization* (Springer-Verlag New York, 2006).
- ³⁵S. Schuster, C. Hilgetag, J. H. Woods, and D. A. Fell, “Elementary modes of functioning in biochemical replicators,” in *Computation in Cellular and Molecular Biological Systems* (Singapore: World Scientific, 1996) pp. 151–165.
- ³⁶Graph cycle are understood as closed paths in the graph, and should not be confounded with reaction cycles.
- ³⁷R. Breslow, *Tetrahedron Lett.* **21**, 22 (1959).
- ³⁸A. Ricardo, F. Frye, M. A. Carrigan, J. D. Tipton, D. H. Powell, and S. A. Benner, *J. Org. Chem.* **71**, 9503 (2006).
- ³⁹A. J. P. Teunissen, T. F. E. Paffen, I. A. W. Filot, M. D. Lanting, R. J. C. van der Haas, T. F. A. de Greef, and E. W. Meijer, *Chem. Sci.* **10**, 9115 (2019).
- ⁴⁰Containing only one fork.
- ⁴¹V. Vasas, C. Fernando, M. Santos, S. Kauffman, and E. Szathmáry, *Biol. Direct* **7**, 1 (2012).
- ⁴²S. A. Kauffman, *A world beyond physics: the emergence & evolution of life* (Oxford University Press, 2019).
- ⁴³J. Chen, S. Körner, S. L. Craig, S. Lin, D. M. Rudkevich, and J. Rebek, *Proc. Natl. Acad. Sci. U. S. A.* **99**, 2593 (2002).
- ⁴⁴G. King, *BioSystems* **15**, 89 (1982).
- ⁴⁵E. Szathmáry, *Philos. Trans. R. Soc. B Biol. Sci.* **355**, 1669 (2000).
- ⁴⁶S. Karlin and H. M. Taylor, *A first course in stochastic processes* (Academic Press, New York, 1975).
- ⁴⁷Note that in general, the calculation of P_{ex} may involve reactions that are not in the core. Here we consider sufficiently simple cases where this is not necessary.
- ⁴⁸á. Kun, B. Papp, and E. Szathmáry, *Genome Biol* **9**, R51 (2008).
- ⁴⁹Andersen, J. L. and Flamm, C. and Merkle, D. and Stadler, P. F., *IEEE/ACM Trans. Comput. Biol. Bioinform* **16**, 510 (2017).
- ⁵⁰R. Milo, S. Shen-Orr, S. Itzkovitz, N. Kashtan, D. Chklovskii, and U. Alon, *Science* **298**, 824 (2002).
- ⁵¹D. Grey, V. Hutson, and E. Szathmáry, *Proc. R. Soc. Lond. B* **262**, 29 (1995).
- ⁵²A. Blokhuis, P. Nghe, L. Peliti, and D. Lacoste, *J. Theor. Biol.* **487**, 110110 (2020).
- ⁵³Halpern, J. J. *Electrochem. Soc.* **100**, 421 (1953).
- ⁵⁴R. Krishnamurthy, *Chem. Eur. J.* **24**, 16708 (2018).
- ⁵⁵K. Andersson, G. Ketteler, H. Bluhm, S. Yamamoto, H. Ogasawara, L. G. M. Pettersson, M. Salmeron, and A. Nilsson, *J. Am. Chem. Soc.* **130**, 2793 (2008).
- ⁵⁶D. Angeli, P. D. Leenheer, and E. D. Sontag, *Math. Biosci.* **210**, 598 (2007).
- ⁵⁷J. Chen, S. Körner, S. L. Craig, D. M. Rudkevich, and J. Rebek, *Nature* **415**, 385 (2002).
- ⁵⁸G. King, *J. Theor. Biol.* **123**, 493 (1986).
- ⁵⁹Provided we choose $1 \leq k \leq m - n$.

SUPPLEMENTARY INFORMATION

I. TERMINOLOGY

A. IUPAC Definitions

To promote the consistent use of terminology, IUPAC committees establish recommendations which serve as a basis for the Compendium of Chemical Terminology (*The Gold Book*), of which some relevant entries are reproduced here. Comments in italic have been added for clarity.

Chemical Reaction: A process that results in the interconversion of chemical species. Chemical reactions may be elementary reactions or stepwise reactions. (It should be noted that this definition includes experimentally observable interconversions of conformers.) Detectable chemical reactions normally involve sets of molecular entities as indicated by this definition, but it is often conceptually convenient to use the term also for changes involving single molecular entities (i.e. 'microscopic chemical events').

Catalyst: A substance that increases the rate of a reaction without modifying the overall standard Gibbs energy change in the (*net*) reaction; the process is called catalysis. The catalyst is both a reactant and product of the (*catalyzed*) reaction. The words catalyst and catalysis should not be used when the added substance reduces the rate of reaction (see inhibitor). Catalysis can be classified as homogeneous catalysis, in which only one phase is involved, and heterogeneous catalysis, in which the reaction occurs at or near an interface between phases. Catalysis brought about by one of the products of a (*net*) reaction is called autocatalysis. Catalysis brought about by a group on a reactant molecule itself is called intramolecular catalysis. The term catalysis is also often used when the substance is consumed in the (*net*) reaction (for example: base-catalysed hydrolysis of esters). Strictly, such a substance should be called an activator.

Autocatalytic Reaction: A (*net*) chemical reaction in which a product (or a reaction intermediate) also functions as a catalyst. In such a reaction the observed rate of reaction is often found to increase with time from its initial value.

B. Allocatalysis

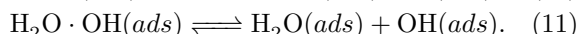
We refer to allocatalysis as the form of catalysis in which, at the end of a catalytic cycle, the catalyst(s) have not changed in number. By their equal participation in either direction, allocatalysts will thus drop out of the net reaction. Some authors refer to autocatalysis as homocatalysis and allocatalysis as heterocatalysis, which is a lexicologically consistent choice of terms

that express an opposition (same vs different). This opposition between same and different is e.g. found in the IUPAC terminology for a homogeneous catalysis (occurring in the same phase) and heterogeneous catalysis. For the IUPAC recommended terminology 'autocatalysis', a consistent choice that expresses this opposition is 'allocatalysis' (self vs other).

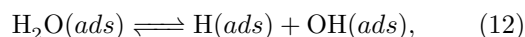
C. Remarks

1. Directionality of autocatalysis

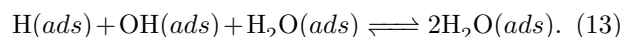
In an allocatalytic reaction, catalysts are produced and consumed in equal amount, and both the 'forward' or 'backward' are accelerated, independently of whether the reaction goes in one or the other direction. In contrast, the term autocatalysis only applies in one direction, due to the requirement of having catalysts be the product of the net reaction. However, the reaction in the other direction is still a form of catalysis, sometimes referred to as 'reverse autocatalysis'. For example, water adsorbed on a copper surface $\text{H}_2\text{O}(\text{ads})$ can strongly accelerate its own disproportionation⁵⁵.



In this direction, the net reaction produces no catalysts (instead, it degrades them):



hence it does not satisfy the stoichiometric requirements for autocatalysis. However, in the opposite sense an appropriate stoichiometry for autocatalysis can be realized:



Note that reaction (11) is still a form of catalysis: H_2O is a reactant and product in reaction (11), which represents an accelerated pathway for reaction (12).

2. Inhibition

A compound is a catalyst in the context of a particular experimental condition where it accelerates the rate of a reaction. A change of those conditions may change this label, the compound may become an in-

hibitor instead. E.g. consider



For a rate acceleration to occur, steps 2,3,4 must together proceed faster than reaction 1. Template-assisted ligation of DNA or RNA provides an example where this may not be the case: below a critical annealing temperature the detachment of the product (here, AB in step 4) becomes increasingly slower for longer strands, and the template becomes an inhibitor.

3. Autonomy and siphons

The concept of autonomy is closely related to the concept a siphon in Chemical Reaction Networks (CRN) theory⁵⁶: A *Siphon* Σ is a subset $\Sigma \subset \mathcal{S}$ of all species S , which for each reaction that has a species in Σ as a product, has at least one of its reactants in Σ .

In this definition, a reaction can be irreversible in a mathematical sense: the reverse reaction does not exist. For a reversible CRN, a reverse reaction does exist, and the siphon definition must apply to the forward and backward direction, thus becomes equivalent to autonomy. A reaction must then imply both one or more products and one or more reactants from Σ (siphon reactions), or none at all (external reactions). Note that autonomy is less restrictive than the conditions posed in Barenholz et al.²⁸, where in addition species must be both reactant and product of a reaction. This last conditions is a proved as a consequence for minimal structures in our choice of formalism (see below).

II. MATHEMATICAL DERIVATION OF AUTOCATALYTIC CORES

A. Reaction graph definitions

Reaction graphs described below correspond to weighted directed hypergraphs without self-loops in the language of graph theory. In this section, the word *cycle* is used in the sense of graph theory (see below), not in the sense of *reaction cycle* used to denote right null-vectors of the stoichiometric matrix. In the following, letters used for scalars indicate positive numbers, and cycles and paths are understood as directed.

Definition 1. A *reaction graph* \mathcal{H} is a triplet (S, R, M) where $\{s_1, \dots, s_n\}$ is the species set, $R =$

$\{r_1, \dots, r_m\}$ is reaction set, each r_j being an ordered pair (X_j, Y_j) of non-empty and non-intersecting subsets of S respectively called reactants and products, and M is the stoichiometric matrix with coefficients m_{ij} . $m_{ij} = 0$ when the species s_i does not participate to the reaction r_j , $m_{ij} < 0$ when species s_i is a reactant of r_j , and $m_{ij} > 0$ when species s_i is a product of r_j .

The stoichiometric matrix M contains all the information about the hypergraph, the column of M corresponding to reactions, and the rows to species.

Definition 2. A *subgraph* of $\mathcal{H} = (S, R, M)$ is a triplet $\mathcal{H}' = (S', R', M')$ where S' is a subset of S , R' is a set of reactions which reactants and products are in S' and intersect the reactant set and product set of a reaction in R , with corresponding stoichiometric coefficients M' .

Definition 3. A reaction graph is *square* if it has the same number of reactions and species.

Definition 4. A *directed path* is a sequence of alternating species and reactions, all reactions and species being distinct, where species which precede and succeed a reaction are respectively a reactant and a product of it. A path is a *minimal path* if it is not possible to form a path starting and ending at the same species using a strict subset of its reactions. A path is *semi-open* if it either starts or ends with an edge.

Definition 5. In a directed path, an edge has a *back-branch* if one of its products is a species located upstream in the path, and this product is called a back-product. An edge has a *forward-branch* if one of its reactants is a species located downstream in the path, and this product is called a forward-reactant.

Definition 6. A *cycle* has an identical definition as a path, except that the first and last species are the same species. A cycle is minimal if it is not possible to form a cycle with a subset of its species and reactions.

Definition 7. A species S is the *solitary* reactant (product) of a reaction if S is the only reactant (resp. product) of this reaction, otherwise it is a *co-reactant* (resp. co-product).

Definition 8. A reaction is *simple* if has a single reactant and a single product.

Definition 9. Consider a simple reaction R with reactant x and product y , with respective stoichiometries $-a$ and b . The *contraction* of R consists of: (i) removing R ; (ii) merging x and y into a single species z , and; (iii) multiplying by a (resp. b) the stoichiometric coefficients associated with z for all reactions formerly associated with x (resp. y).

Definition 10. In a square graph, a *perfect matching* is a bijection between species and reactions. It corresponds to all pairs $(i, \sigma(i))_{i=1 \dots N}$, where i is the

index of a species, σ is a permutation of $[1\dots N]$, and $\sigma(i)$ is the index of a reaction. A perfect matching of a graph, or a subgraph, \mathcal{G} is called a \mathcal{G} -matching.

Remarks:

- Consider reactions $E = (\{a\}, \{b, c\})$ and $F = (\{b\}, \{c\})$; $a - E - b - F - c$ is a path, but it is not minimal because it contains $a - E - c$. Simple paths are necessarily minimal (Fig. S1a).
- Consider $E = (\{a\}, \{b\})$ and $F = (\{b\}, \{a, c\})$; $a - E - b - F - c$ is a minimal path and F has a back-branch (Fig. S1a). In particular, it contains a cycle $a - E - F - a$.
- Simple paths are exactly cycle-free minimal paths.
- More generally, a minimal path can have back-products and forward-reactants (Fig. S1a).
- A hypergraph cycle can have reactions connecting several of its species, but a minimal cycle cannot. Thus, a minimal cycle only contains simple paths (it is identical to a cycle in a regular graph).
- Cycles are square.

B. Relationship with linear algebra

$x \succ 0$ denotes a real vector with only strictly positive coordinates.

Definition 11. A matrix M is **productive** if there exists a real vector γ such that $M \cdot \gamma \succ 0$. Equivalently, M intersects the strictly positive orthant $\mathbb{R}_{>0}^n$.

Definition 12. A matrix is **autonomous** if its columns all contain a strictly negative and a strictly positive coefficient.

Definition 13. A minimal cycle is **weight-symmetric** if the product of the absolute values of the stoichiometric coefficients associated with its reactants equals the product of the stoichiometric coefficients associated with its products. Otherwise, the cycle is **weight-asymmetric**.

Remarks:

- Autonomous matrices are stoichiometric matrices of reactions systems such that every reaction has at least one reactant and at least one product.
- The Leibniz formula for the determinant shows that the non-zero terms of $\det(M)$ exactly correspond to the products of stoichiometric coefficients $m_{i, \sigma(i)}$ determined by each possible perfect matching of the graph.

- A minimal cycle \mathcal{C} has exactly two perfect matchings, which correspond to the matching of its reactions with their solitary reactants and solitary products respectively. $\det(\mathcal{C}) = 0$ if and only if \mathcal{C} is weight-symmetric.

- Be \mathcal{H}' the hypergraph obtained from \mathcal{H} by contracting a simple reaction R . The cofactor expansion implies that $|\det(\mathcal{H}')| = |\det(\mathcal{H})|$. Additionally, any cycle \mathcal{C} of \mathcal{H} becomes a cycle \mathcal{C}' in \mathcal{H}' obtained by contracting R , and $|\det(\mathcal{C}')| = |\det(\mathcal{C})|$.

C. Autocatalytic cores

Definition 14. A **core** is a minimal productive reaction graph, i.e. a reaction graph that does not contain any productive subgraph.

Finding cores is equivalent to finding minimal matrices which are productive and autonomous. In this section, we denote $M \in \mathbb{R}^{n,m}$ the stoichiometric matrix of the graph \mathcal{H} , where n is the number of rows (species) and m the number of columns (reactions). If M is productive, we denote γ a vector such that $M \cdot \gamma \succ 0$. Productivity of M is indifferent to the sign of its columns as the sign of the coefficients of γ is not constrained. Therefore, we choose the convention that any productive vector γ is positive, up to taking the opposite for some columns of M .

Remarks:

- M invertible implies M productive, as the image of M is then the full space $\mathbb{R}^{n,m}$, which contains the strictly positive orthant.
- Below, species or reactions 'can be removed' is understood as 'can be removed while preserving productivity and autonomy'. Being able to remove a row (a species) or a column (a reaction) contradicts the minimality of a core.
- Removing columns (reactions) preserves autonomy, but not necessarily productivity.
- Removing rows (species) preserves productivity, but not necessarily autonomy.
- A row corresponding to a species that is always a co-reactant or a co-product can be removed without affecting autonomy (every column still contains positive and negative coefficients) and productivity.

Proposition 1. In a core, every species is both a reactant and a product.

Proof. Every species must be produced, otherwise it would not be possible to find a positive γ verifying $M \cdot \gamma \succ 0$. Now, suppose a species S is never a reactant

and only a product. All reactions such that S is their only product can be removed without affecting the productivity of other species. In the resulting graph, either S is not the product of any reaction anymore, or S is only a co-product of the remaining reactions. In both cases, S can be removed without affecting autonomy. \square

Proposition 2. *A core is square, invertible, every species is the solitary reactant of a reaction, and is reactant for this reaction only.*

Proof. Consider $M \in \mathbb{R}^{n,m}$ a productive stoichiometric matrix with n species and m reactions, with rank k . Obviously $k \leq m, n$. We must also have $m = k$, otherwise a column could be removed while preserving the image of M , thus productivity. Additionally, every species must be the solitary reactant of at least one reaction, otherwise it could be removed. This implies $m \geq n$. Overall, $k = m \geq n \geq k$, so that $k = m = n$, meaning that M is square and invertible. As every species S is the solitary reactant of at least one reaction R and $m = n$, the species is a reactant for only R . \square

Remark: Property 2 implies that M can be rearranged in such a way that it has a strictly negative diagonal, and only non-negative off-diagonal coefficients.

Proposition 3. *In a core, a square autonomous submatrix must have a product outside its set of species.*

Proof. Be A a square autonomous submatrix of M and write $M = \begin{pmatrix} A & C \\ B & D \end{pmatrix}$. We need to show that $B > 0$. As A is autonomous, every A -reaction has a reactant in the set of A -species. By Property 2, reactants are always solitary, thus $B \geq 0$. Now suppose $B = 0$. Then $\det(M) = \det(A) \cdot \det(D)$. Either $\det(A) = 0$, implying $\det(M) = 0$, contradicting M invertible, or $\det(A) \neq 0$, then A is productive, contradicting the minimality of M . \square

Proposition 4. *A core is strongly connected.*

Proof. Consider a species x_0 of M . Below, we recursively construct sets $D_k = \{x_1, \dots, x_k\}$ of increasing cardinal, such that every x_i is downstream x_0 , until $k = n - 1$, implying that for any species $y \neq x$, there exists a path from x to y . We denote $R(S)$ the only reaction with reactant S , which is well defined by Property 2. **Step 1:** We take x_1 as a product of $R(x_0)$. **Step k:** Suppose D_k exists, $k < n - 1$. Re-arrange M such the top left block A of size k corresponds to species set D_k and reaction set $R(D_k)$. As A is autonomous, by Property 3, there exists a species x_{k+1} outside of D_k which is downstream D_k , hence D_{k+1} exists. \square

Proposition 5. *In a core, every species is involved in a cycle.*

Proof. Obvious from Property 4, considering the back and forth paths joining any two species. \square

Proposition 6. *Consider a partition of a core into two species sets V and W . V cannot be upstream of W , i.e. reactions with products in W cannot have all their reactants in V .*

Proof. Suppose on the contrary that M can be written $M = \begin{pmatrix} A & B \\ 0 & C \end{pmatrix}$ where A and B span V , C spans W , and $B \leq 0$. Given the latter inequality, Property 1 implies that A is non-empty and autonomous. Consider $\gamma > 0$ such that $M \cdot \gamma \succ 0$. Be α and β the respective restrictions of γ to the reaction spaces of A and B . Then $A \cdot \alpha + B \cdot \beta \succ 0$. As $B \cdot \beta \leq 0$, we have $A \cdot \alpha \succ 0$, contradicting the minimality of M . \square

The definitions below are generalizations of the notion of ear decomposition in regular graphs (Fig. S1b).

Definition 15. A **hyper-ear** is a hypergraph comprising a minimal cycle \mathcal{C} , called the base cycle, such that \mathcal{C} has a reaction with a product x outside \mathcal{C} , and a minimal path \mathcal{P} starting at x , such that its last reaction, R , has a product in \mathcal{C} , R being the only \mathcal{P} -reaction to have a product in \mathcal{C} . A **proto-ear** has a similar definition, but where \mathcal{C} is a simple path (called the base path) instead of a minimal cycle.

Description of proto-ears and hyperears - In a hyper-ear or a proto-ear, any \mathcal{C} -reaction can have x as a product, and any \mathcal{C} -species can be the product of R , the last reaction of \mathcal{P} (Fig. S1b). We denote by u a species which is the product of R , v any \mathcal{C} -species which is the reactant of a \mathcal{C} -reaction which produces x , ' $-$ ' a simple path (including the empty path), o a simple path comprising at least one species, o being a subcase of the ' $-$ ' category. By convention, a uv motif can correspond to a single same species which is both a R -product and a reactant for x production. Any proto-ear falls into a class described by a chain made of the symbols u , v , o , and ' $-$ ', as soon as it contains at least a u and a v . Reciprocally, any such chain represents one or more proto-ears. Any hyper-ear is obtained by cyclic closure of the base path of a proto-ear. Such closure is denoted by the '*' symbol at the beginning and the end of the chain.

Theorem 1. *Cores are of one of the following types:*

- **TYPE I:** a weight-asymmetric minimal cycle;
- **TYPE II:** a cycle comprising all species as solitary reactants, and one or more weight-symmetric sub-cycles without intersection between them;

- *TYPES III-IV-V: one of the three types of hyper-ears, any subcycle of which is weight-symmetric: (III) $*u-v-o*$; (IV) $*u-u-v*$; (V) $*u-v-u-v*$.*

Proof. Core type are represented in Fig. S1c. \mathcal{H} denotes the reaction graph and M its stoichiometric matrix.

SUFFICIENCY

Step 1: All types have a non-zero determinant.

TYPE I: Invertibility is a direct consequence of the remark on the determinant of minimal cycles.

TYPE II: Consider a minimal weight-symmetric subcycle \mathcal{C} of \mathcal{H} . Any \mathcal{H} -matching consistent with a \mathcal{C} -matching can be associated to another \mathcal{H} -matching obtained by reversing the \mathcal{C} -matching. Thus, $\det(\mathcal{H})$ has the form $\det(\mathcal{C})\alpha + \beta$, where the first term comprises all \mathcal{C} -consistent \mathcal{H} -matchings. As $\det(\mathcal{C}) = 0$, it suffices to show that β is a single non-zero term. By Property 3, \mathcal{C} must have a reaction R_1 with a product x_1 outside of \mathcal{C} . As by definition of TYPE II, subcycles are non-intersecting, R_1 must be the only \mathcal{C} -reaction with a product outside \mathcal{C} , and x_1 must be the only product of R_1 outside \mathcal{C} . All non-zero terms in β require matching R_1 to x_1 , otherwise R_1 would be matched with a \mathcal{C} -species, which would impose a \mathcal{C} -matching (\mathcal{C} being a minimal cycle), contradicting the definition of β . We now order the indexes k following the downstream order of the x_k species along \mathcal{H} , and show recursively that β corresponds to the \mathcal{H} -matching where every R_k matches x_k : (step 1) By construction, R_1 matches x_1 . (step k) Suppose R_{k-1} matches x_{k-1} . Either R_k is a simple reaction, and, as its reactant x_{k-1} is already matched, R_k necessarily matches its only product x_k . Or R_k has a back-branch forming a minimal cycle. However, cycles are non-intersecting, so that the back-product x_i of R_k is necessarily downstream x_k and upstream x_{k-1} , thus x_i is already matched by the recursion hypothesis. Thus, R_k can only match x_k .

TYPES III-IV-V: Consider the stoichiometric matrix M with non-negative off-diagonal coefficients:

$$M = \begin{pmatrix} -1 & c & e \\ a & -1 & f \\ b & d & -1 \end{pmatrix} \quad (18)$$

We have $\det(M) = -1 + df + ac + ade + bcf + be$. Strict subcycles must be weight-symmetric, as otherwise, the minimality of M would be contradicted. Consequently, when their factors are both non-zero, the products df , ac , and be must be equal to 1. By contracting all simple reactions and multiplying the columns of M if necessary so that solitary reactant stoichiometries are all normalized to -1 , TYPE III corresponds to $d = f = 0$ and $a, b, c, e > 0$, TYPE IV to $f = 0$ and $a, b, c, d, e > 0$, and TYPE V to all coefficients

strictly positive. In all these cases, we have $\det(M) > -1 + ac + be = 1$.

Step 2: All types are minimal

TYPE I: Removing any subset of species or reactions would result in an acyclic graph, contradicting Property 5.

TYPE II: Removing any subset of species or reactions either leads to a hypergraph where a subset of species is upstream the rest, contradicting Property 6, or to a non-invertible minimal cycle.

TYPE III-V: Removal of any set of reactions (and a fortiori of species, given that they all are solitary reactants) leaves at most one cycle in the graph, the latter being non-invertible.

NECESSITY

By Property 5, there exists a minimal cycle \mathcal{C} in \mathcal{H} . Either \mathcal{C} is weight-asymmetric, then $\mathcal{H} = \mathcal{C}$ is of TYPE I. Or \mathcal{C} is weight-symmetric. Then, by Property 3, there is a \mathcal{C} -reaction with a product x outside \mathcal{C} . By Property 4, there exists a path \mathcal{P} from x to any species in \mathcal{C} (Fig. S1d). We can take \mathcal{P} minimal and such that only its last reaction has a product in \mathcal{C} , thus forming a hyper-ear $*mu - vm*$ where m symbols stand for any other hyper-ear motif. Below, we show that hyper-ears are either one of the types II-V, or contain a TYPE II, III or IV core as a subgraph, overall demonstrating that \mathcal{H} is necessarily a hyper-ear of TYPE II-V. \square

Before continuing the proof of the theorem, we show an additional property based on the sufficiency of TYPE I and TYPE III.

Proposition 7. *In a core, a minimal path can have back-branches but no forward-branch, and the cycles formed by back-branches are non-intersecting.*

Proof. Consider a minimal path \mathcal{P} in a core \mathcal{H} . Forward-branches require reactions to have multiple reactants, contradicting Property 1. Therefore, \mathcal{P} is either a simple path or it has back-branches. Suppose there exists two back-products y and z of the respective reactions r_y and r_z , respectively forming intersecting cycles \mathcal{C}_y and \mathcal{C}_z (Fig. S1e). Without loss of generality, y and z can be taken closest, y upstream of z , and such that there is no other cycle nested within \mathcal{C}_y and \mathcal{C}_z than possibly themselves. \mathcal{C}_z is necessarily weight-symmetric, as it would otherwise contradict the minimality of \mathcal{H} . There are two cases. Case 1: r_z is upstream r_y (\mathcal{C}_z is nested within \mathcal{C}_y). Call \mathcal{P}' the path from the product of r_z to r_y then y then z . Then \mathcal{C}_z and \mathcal{P}' form a TYPE III core. Case 2: r_y is upstream r_z (\mathcal{C}_z and \mathcal{C}_y are entangled). Call \mathcal{P}' the path joining y to z . Then \mathcal{C}_z and \mathcal{P}' form a TYPE III core. Overall, we have shown that the existence intersecting cycles along a minimal contradicts the minimality of \mathcal{H} . \square

We now go back to the proof of the theorem.

Proof. Consider the minimal path \mathcal{P} of the hyper-ear, where \mathcal{P} starts at x . By Property 7, \mathcal{P} has no forward-branch.

Case A (TYPE II): Suppose \mathcal{P} has one or more back-branch. Consider a reaction R' of \mathcal{P} which has a back-branch, with back-product y' and forming a cycle \mathcal{C}' . \mathcal{C}' is necessarily weight-symmetric by minimality of \mathcal{H} . Call x' the product of R' outside \mathcal{C}' . Consider the path \mathcal{P}' starting at x' , then going downstream of \mathcal{P} until it reaches a shortest subpath $u-v$ of \mathcal{C} , then to x , and finally from x to y' in \mathcal{P} . By Property 7, all cycles along \mathcal{P} are non-intersecting, and by construction, \mathcal{C} is non-intersecting with the cycles of \mathcal{P} . Consequently, \mathcal{P}' only has non-intersecting cycles, so that \mathcal{C}' and \mathcal{P}' form a TYPE II motif. Thus, the base cycle of the hyper-ear cannot have species outside $u-v$, as otherwise the core made of \mathcal{C}' and \mathcal{P}' would be a strict subset of \mathcal{H} , contradicting its minimality. This shows that \mathcal{H} is a $*u-v*$ hyper-ear with a minimal path comprising non-intersecting cycles, the latter being necessarily weight-symmetric. Thus \mathcal{H} is a TYPE II core.

Case B (TYPES III-V): Suppose \mathcal{P} has no back-branch, in other words \mathcal{P} is a simple path.

Subcase B.1 (TYPE III): Suppose \mathcal{H} a hyper-ear which has only one u and one v symbol, thus a $*u-v*$ hyper-ear. The case $*u-v*$ with a simple path is covered by the definition of TYPE II. If the $'-'$ symbol does not represent an empty path, then it comprises at least one species, so that \mathcal{H} is a $*u-vo*$ hyper-ear with simple path \mathcal{P} , corresponding to TYPE III.

Subcase B.2 (TYPE IV): Suppose the hyper-ear comprises one u or v symbol in addition to the $u-v$ motif. We first note that $u-u-v$ and $u-v-v$ proto-ears are isomorphic to $*u-v*$, which falls into the categories of TYPE II or TYPE III cores. Therefore, in a core, a hyper-ear containing two successive u or v symbols is necessarily of the form $*u-u-v*$ or $*v-v-u*$, or their cyclic permutations, as any additional symbol would allow to find a strict subgraph $u-u-v$ or $u-v-v$ forming a core, contradicting the minimality of \mathcal{H} . Furthermore, $*u-u-v*$ and $*v-v-u*$ hyper-ears are isomorphic. Indeed, the matrices of their reduced forms correspond to the matrix shown in the SUFFICIENCY section of the theorem, where exactly one coefficient is set to zero. Thus, these motifs as well as all their cyclic permutations, fall into the category of TYPE IV.

Subcase B.3 (TYPE V): Subcase B.2 imposes that any motif containing four or more u or v symbols must alternate u and v symbols. Any motifs with five or more u or v symbols contains, up to permutation, a $u-v-u-v$ proto-ear as a strict subgraph. However, the latter is isomorphic to TYPE IV cores, which implies that $*u-v-u-v*$ (TYPE V) is the only motif in this class which does not contradict the minimality of \mathcal{H} .

III. CHEMICAL INTERPRETATION OF AUTOCATALYTIC CORES

We remind that the notion of 'graph cycle' (closed successions of nodes and edges) differs from the notion 'reaction cycle' (right null vectors of the stoichiometric matrix). The latter name was historically chosen because the two notions overlap in the particular case of the simplest catalytic cycles, but there are counterexamples for both (we give one later). We employ 'reaction cycle' and 'graph cycle' to distinguish these notions.

By the minimality of autocatalytic cores, an autocatalytic motif is either a core, or it contains one or several cores. If P is a property of cores, then for any autocatalytic motif, either it verifies P , or it contains an autocatalytic motif verifying P . In particular,

- by Property 1, every autocatalytic motif contains an invertible autocatalytic motif;
- by Property 2, every autocatalytic motif contains an autocatalytic motif such that every product is also a catalyst of the reaction, or equivalently, such that every species appears on both side of the total chemical equation.

The five categories of cores are schematically represented in Fig. S1c. The convention of representation are as follows. The edges of the graph correspond to reactions and the yellow nodes to species. Reaction have two sides, the reactant side and product side, and each side of the edge representing the reaction connects to one or several nodes representing the species, with a stoichiometry for each connection. In the Type I core, the edge from the top node to the bottom node ends with a fork, the two ends of which connect to a single bottom node (S1c). This means that the bottom species is produced with a stoichiometry of 2 by this reaction. For simplicity, we have represented the connection between all other edges and nodes without fork. However, in all generality, any connection between an edge and a node could be a fork (e.g. could be of stoichiometry >1), as soon as the rules on graph cycle symmetry are respected, as explained below. Forks also appear in Types II-V, but where they connect to two distinct nodes, which are two distinct product species. The orange squares indicate that the reaction represented can be replaced by a chain of reactions with a single reactant species and a single product species.

The mathematical derivations are done without constraint on the number of reactants or products a reaction step can have. However, in a chemical system, elementary reactions are in principle either unimolecular or bimolecular. This restricts the range of possible

core graphs. This restriction operates only at the level of the stoichiometry of each single reaction, not at the level of the overall structure of cores. Indeed, even without invoking the restriction on bimolecularity, the mathematical derivation results in cores such that every reaction step involves at most a single species as reactant and at most two species as products, so that bimolecularity can always be respected, provided rules on the stoichiometry of each connection.

In a chemical autocatalytic core, an edge with a fork connecting to two distinct nodes (e.g. a reaction with two distinct product species) must have a stoichiometry 1 for each connection in order to respect bimolecularity. If a reaction has only one product species, then its stoichiometry can be 1 or 2, as soon as it respects rules on cycle stoichiometry, which we detail now.

Consider a simple graph cycle \mathcal{C} , simple meaning that every reaction as a single reactant species and a single product species. Note a_i (resp. b_i) the stoichiometry of the reactant (resp. product) of reaction i . If $\prod_i a_i \neq \prod_i b_i$, we say that \mathcal{C} is weight-asymmetric, otherwise it is weight-symmetric. Weight-asymmetric simple graph cycles are an example of graph cycle which has no reaction cycle. Weight-symmetric graph cycle taken in isolation have a reaction cycle (their determinant is zero as shown in the derivation of cores above), thus they correspond to allocatalytic cycles in the context of a larger reaction graph where the reactions of the graph cycle consume and/or produce species outside of its own species set. The most classical example of an allocatalytic cycle is represented in Fig S1f, where reactant S is provided from the environment, binds to catalyst E to form complex ES converted into EP, finally dissociated into E which is recycled, and product P.

Type I cores are weight-asymmetric simple graph cycles, as \mathcal{C} in S1c. Consequently, in Types II-V, any simple graph cycle must be weight-symmetric (these graph cycles correspond to reaction cycles), otherwise the core would contain a Type I core, contradicting its minimality. For example in S1c: in Type II, \mathcal{C} must be symmetric, but this does not apply to \mathcal{C}' because it is not even a simple cycle; in Types III-V, \mathcal{C} , \mathcal{C}' and \mathcal{C}'' must be symmetric. Type II cores consist of a large graph cycle (\mathcal{C}' in Fig S1c) comprising smaller graph cycles embedded within it (for example \mathcal{C} in Fig S1c). Given the above, each of these smaller cycles must be weight-symmetric, and obeys the definition of an allocatalytic cycle. The Type II category includes circularly closed successions of such allocatalytic cycles, where the product of one allocatalytic cycle is the catalyst of the next allocatalytic cycle, which is a typical example of autocatalytic set. In addition however, Type II allows intermediate non catalyzed reaction steps.

Notably, every core follows the basic structure

represented on Fig S1d, comprising a base cycle \mathcal{C} and a minimal path (in the sense of reaction hypergraphs, see former section) starting from a reaction fork and joining back to a node of \mathcal{C} . This structure should enable a systematic algorithmic search for autocatalytic motifs in large stoichiometries.

IV. EXAMPLES AND APPLICATION OF THE STOICHIOMETRIC CRITERIA

A. Example of autocatalytic submotif

We illustrate the concepts of autocatalytic submotif and the properties demonstrated above on a toy model for the Formose reaction, to which we have added one auxiliary reaction $C_3 \rightleftharpoons D_3$, so that we obtain a stoichiometric matrix

$$\nu = \begin{matrix} & \begin{matrix} 1 & 2 & 3 & 4 \end{matrix} \\ \begin{matrix} C_1 \\ C_2 \\ C_3 \\ D_3 \\ C_4 \end{matrix} & \begin{pmatrix} -1 & -1 & 0 & 0 \\ -1 & 0 & 2 & 0 \\ 1 & -1 & 0 & -1 \\ 0 & 0 & 0 & 1 \\ 0 & 1 & -1 & 0 \end{pmatrix} \end{matrix} \quad \begin{matrix} C_1 + C_2 \xrightarrow{1} C_3 \\ C_1 + C_3 \xrightarrow{2} C_4 \\ C_4 \xrightarrow{3} 2C_2 \\ C_3 \xrightarrow{4} D_3 \end{matrix} \quad (19)$$

this full matrix has a left nullvector $\mathbf{l} = (1, 2, 3, 3, 4)$, i.e. we have a mass-like conservation law

$$L = n_{C_1} + 2n_{C_2} + 3n_{C_3} + 3n_{D_3} + 4n_{C_4}. \quad (20)$$

Thus, this matrix does not correspond to an autocatalytic motif. Upon removing C_1 (then considered as a feedstock molecule), we obtain an autocatalytic matrix ν_*

$$\nu_* = \begin{matrix} & \begin{matrix} 1 & 2 & 3 & 4 \end{matrix} \\ \begin{matrix} C_2 \\ C_3 \\ D_3 \\ C_4 \end{matrix} & \begin{pmatrix} -1 & 0 & 2 & 0 \\ 1 & -1 & 0 & -1 \\ 0 & 0 & 0 & 1 \\ 0 & 1 & -1 & 0 \end{pmatrix} \end{matrix} \quad \begin{matrix} C_2 \xrightarrow{1} C_3 \\ C_3 \xrightarrow{2} C_4 \\ C_4 \xrightarrow{3} 2C_2 \\ C_3 \xrightarrow{4} D_3 \end{matrix} \quad (21)$$

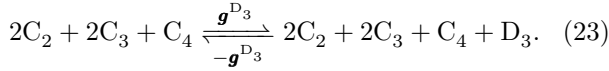
This matrix is autonomous and invertible with inverse:

$$\nu_*^{-1} = \frac{1}{3} \begin{pmatrix} 1 & 2 & 2 & 2 \\ 1 & 1 & 1 & 2 \\ 1 & 1 & 1 & 1 \\ 0 & 0 & 1 & 0 \end{pmatrix} = (\mathbf{g}^{C_2}, \mathbf{g}^{C_3}, \mathbf{g}^{D_3}, \mathbf{g}^{C_4}). \quad (22)$$

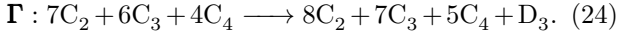
The columns of the inverse are reaction vectors associated to a given species, of which they produce one extra unit. We will refer to them as elementary production modes.

Among the production modes, $\mathbf{g}^{D_3} = (2, 1, 1, 1)^T$ is the sole vector which uses the auxiliary reaction, and

D_3 only ever occurs as a product



If we now consider $\Gamma = g^{C_2} + g^{C_3} + g^{D_3} + g^{C_4}$, we obtain a reaction balance such that every species has a net increase:



ν_* is not minimal as D_3 is only produced, and does not participate as a catalyst. Indeed, Property 2 implies the existence of an autocatalytic submotif without species which does not participate as a catalyst. An autocatalytic submotif is obtained by removing the reaction



and the species D_3 , to obtain the autonomous submatrix $\bar{\nu}$

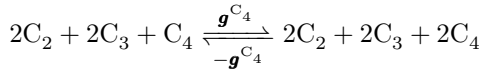
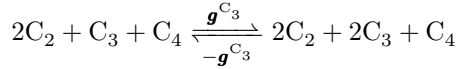
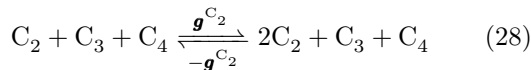
$$\bar{\nu} = \begin{matrix} & \begin{matrix} 1 & 2 & 3 \end{matrix} \\ \begin{matrix} C_2 \\ C_3 \\ C_4 \end{matrix} & \begin{pmatrix} -1 & 0 & 2 \\ 1 & -1 & 0 \\ 0 & 1 & -1 \end{pmatrix} \end{matrix} \quad \begin{matrix} C_2 \xrightleftharpoons{1} C_3 \\ C_3 \xrightleftharpoons{2} C_4 \\ C_4 \xrightleftharpoons{3} 2C_2 \end{matrix} \quad (26)$$

The matrix $\bar{\nu}$ is also invertible

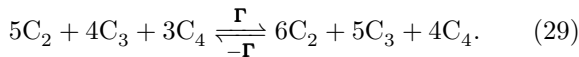
$$\bar{\nu}^{-1} = \frac{1}{3} \begin{pmatrix} 1 & 2 & 2 \\ 1 & 1 & 2 \\ 1 & 1 & 1 \end{pmatrix} = (g^{C_2}, g^{C_3}, g^{C_4}). \quad (27)$$

The columns of $\bar{\nu}^{-1}$ correspond to reaction vectors, whose application yields one net copy of the corresponding molecule, e.g. $\Delta n_k = (\bar{\nu} \cdot g^{(k)})_k = 1$. This is illustrated for C_2 in Fig. S2.

The individual replication cycles are



We can construct $\Gamma = g^{C_2} + g^{C_3} + g^{C_4}$, which leads to the overall reaction

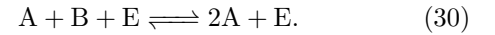


We see here that every species has a net production and is on both sides of the balance, thus participates as a autocatalyst. Furthermore, $\bar{\nu}$ is a Type I core and consequently does not contain any smaller autocatalytic

submotifs.

B. Autoinduction

The concept of autoinduction was put forward by D. Blackmond²⁵, to distinguish between autocatalysis that is mediated by external catalysts (i.e. not part of the autocatalysts that are reproduced) called 'autoinduction', and autocatalysis that functions without the aid of external catalysts (i.e. all catalysts are autocatalysts). We thus obtain a hybrid of pure allocatalysis and autocatalysis, for which the simplest example would be



The IUPAC definitions impose that autoinduction qualifies as autocatalysis. It follows then from our framework that we can find autocatalytic cores in autoinduction networks, which is indeed confirmed in Fig. S3 for the two types of autoinduction that have been proposed²⁵.

The concept of 'autoinduction' addresses a notion of self-sufficiency (also encountered in RAF sets, Sec.IV E): external allocatalysts become essential to successful autocatalysis, yet they are not reproduced. Depending on the context, they could be seen as part of the environment, in the same sense as essential feedstock species. Examples of autoinduction occur in autocatalytic metabolic networks (with locally allocatalytic enzymes) or e.g. the formose reaction which is often catalyzed by base and divalent metal ions.

The presence of external allocatalytic cycles does not add new cycles to the autocatalytic core. A practical consequence is that one can write catalyzed reactions very compactly for the core, while still maintaining nonambiguity, which we make use of in our analysis of metabolic cycles.

C. Metabolic cycles

At least two metabolic cycles are known to be autocatalytic. In our analysis of autoinduction, we pointed out that the core does not contain external allocatalysts (here: enzymes). Written purely in terms of autocatalysts, we find a type II autocatalytic core for the reverse Krebs cycle (Fig. S4a). For the Calvin cycle depicted in Fig. S4b, we identify three Type I cores (two structurally equivalent, differing only in the reaction chosen to link the same core species) and 4 of type II.

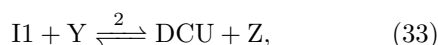
D. Chemical amplification

Chen et al.^{43,57} advanced a general strategy to achieve self-amplifying behavior, demonstrated by the encapsulation of the reactive compound DCC in a cavitand (indicated by an oval around the molecule in EDCC, Fig. S5), which they referred to as chemical amplification. This phenomenon is consistent with the IUPAC definition of autocatalysis, which we will now illustrate by finding its autocatalytic core.

Let us first assess a reaction network formed by two reactions proposed by Chen et al, in absence of the cavitand complexes. In that case, applying our formalism readily reveals that the network cannot exhibit autocatalysis: there are no autocatalytic submatrices.

$$\nu = \begin{matrix} & \begin{matrix} 1 & 2 \end{matrix} \\ \begin{matrix} \text{DCC} \\ \text{X} \\ \text{I1} \\ \text{Y} \\ \text{DCU} \\ \text{Z} \end{matrix} & \begin{pmatrix} -1 & 0 \\ -1 & 0 \\ 1 & -1 \\ 0 & -1 \\ 0 & 1 \\ 0 & 1 \end{pmatrix} \end{matrix} \quad \begin{matrix} \text{DCC} + \text{X} \xrightleftharpoons{1} \text{I1}, \\ \text{I1} + \text{Y} \xrightleftharpoons{2} \text{DCU} + \text{Z}. \end{matrix} \quad (31)$$

Now, let us add the species EDCC and two exchange reactions with DCU and Z that liberate DCC, i.e.



for which we have the matrix

$$\nu = \begin{matrix} & \begin{matrix} 1 & 2 & 3 & 4 \end{matrix} \\ \begin{matrix} \text{DCC} \\ \text{X} \\ \text{I1} \\ \text{Y} \\ \text{DCU} \\ \text{Z} \\ \text{EDCC} \\ \text{EDCU} \\ \text{EZ} \end{matrix} & \begin{pmatrix} -1 & 0 & 1 & 1 \\ -1 & 0 & 0 & 0 \\ 1 & -1 & 0 & 0 \\ 0 & -1 & 0 & 0 \\ 0 & 1 & -1 & 0 \\ 0 & 1 & 0 & -1 \\ 0 & 0 & -1 & -1 \\ 0 & 0 & 1 & 0 \\ 0 & 0 & 0 & 1 \end{pmatrix} \end{matrix} \quad (36)$$

This network admits an autocatalytic submatrix, and we obtain an autocatalytic core of type III consisting of the species DCC, I1, DCU and Z, as can be seen in Fig. S5b. The new reagent EDCC serves as a feedstock compound, that allows to dispense new DCC, that can now serve as an autocatalyst. The generality of the mechanism follows from an exchange that could have been performed with different reactants than DCU and Z to yield an equivalent network, as shown in Refs^{43,57}.

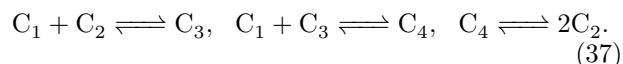
E. Autocatalysis in RAF sets

A definition of Reflexively Autocatalytic Food-generated sets can be found in Ref.²⁴: *a set of reactions \mathcal{R} is RAF if every reaction is catalyzed by at least one molecule involved in a reaction in \mathcal{R} , and every reactant in \mathcal{R} can be constructed from the food set f by successive applications of reactions from \mathcal{R} .* The philosophy behind the RAF set is that 'every reaction' in a RAF-set can be accelerated by the catalysts themselves. RAF sets do not perform autoinduction, except when members of the food set f within a RAF-set also serve as allocatalysts.

In the RAF-set formalism, reaction and catalysis are distinct mathematical objects. Graphically, RAF-sets are typically represented as bipartite graphs (S6a), with nodes (white squares) corresponding to reactions, which connect to nodes (colored circles) which serve as reactants (entering bold arrow) and products (leaving bold arrow) via directed edges. A dashed arrow connecting to a reaction indicates that a species is a catalyst for a reaction. Within the RAF framework, the following terms are employed as distinct: i) autocatalytic reaction ("*is a single chemical reaction for which one of the products also catalyzes the reaction*"), ii) autocatalytic cycle ("*is a sequence of reactions that, once completed, results in two (or more) copies of the molecule that was started with*" such as the toy formose reaction), iii) autocatalytic set (or RAF set).

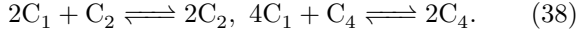
It is important to note that the RAF-set formalism and the distinctions above depend on the chosen level of coarse-graining of the description. In that description (see Fig. S6a) allocatalysts in the same allocatalytic cycle are represented by a single species. The combination of reactions that form the allocatalytic cycle is represented by a single dashed line, connecting to an uncatalyzed reaction. Here, there exists a level of description where a RAF set appears as autocatalytic reaction involving catalytic cycles. By comparing Figs. S6a, we see that the level of description is critical in assessing whether a network is a RAF-set or not. From the definition of a RAF-set, the detailed version of the network in Fig.S6a would not be a RAF, but the less detailed description next to it would be.

Another example is the toy formose reaction, where two different choices of coarse-graining yield two different description in the RAF framework. Even when neglecting the role of catalytic base and metal ions, the toy formose reaction without coarse-graining is not a RAF-set³², since its individual steps are not catalyzed:



Framed solely in terms of C_1 and one autocatalyst (e.g. C_2, C_4) one could propose a description in which we are oblivious of these steps, and write it as an autocatalytic

reaction in the sense of RAF sets, such as



This would work as long as we consider them satisfactory levels of description, depending on the context (e.g. further reactivity of intermediates, separation of timescales): either of these hypothetical cases satisfy the RAF criteria.

An interesting contrast occurs between RAF sets and our formalism: RAF-sets require a level of coarse-graining without intermediates to define catalysis in terms of single catalysts, which ensures a compact and unique description. Our formalism requires each catalytic cycle to have at least one intermediate to satisfy nonambiguity. Although less compact, the description is flexible: adding further steps is always possible and does not alter the conclusions, which must remain in accord with chemical definitions.

In describing catalysis in terms of uncatalyzed reactions, it becomes possible to formalize the underlying structure of catalysis in different models. We will now illustrate how this formally establishes that all autocatalysis in the GARD model qualifies as a RAF-set.

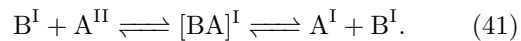
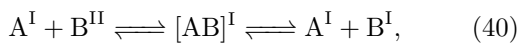
F. GARD model

GARD stands for graded autocatalysis replication domain²², and is a model for the autocatalytic assembly of amphiphile assemblies (e.g. micelles). It describes micelles with a composition $\mathbf{n} = \{n_1, \dots, n_s\}$, that follow an evolution equation

$$\frac{dn_i}{dt} = (k_i^+ \rho_i N - k_i^- n_i) \left(1 + \frac{1}{N} \sum_{j=1}^s \beta_{ij} n_j \right). \quad (39)$$

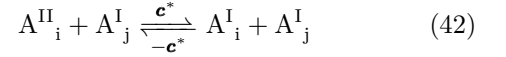
The surfaces are in contact with a reservoir, that contains species Z_i at concentration ρ_i and that can enter the surface, which has an area proportional to N . The incorporation happens with a base rate of k_i^+ , but can be facilitated by other amphiphiles, for which the catalytic rate enhancement is characterized by β_{ij} . A special ingredient in GARD is the division process, which splits a mature surface in two new ones, after achieving a maximal size.

We examine here stoichiometric mechanisms leading to Eq. (39). Let us consider amphiphiles A and B, which can be in the micelle or reservoir, labelled I and II (see Fig. S6). To catalyze incorporation of the other, a complex is formed with a reservoir species, and subsequent dissociation takes place in the micelle



This network corresponds exactly to the network discussed in Fig. S6a, where the products of two allocatalytic cycles serve as a catalyst for each other, a Type II core in our stoichiometric formalism.

More generally, labelling amphiphiles as A_k ($k \in \{1, 2, \dots, s\}$), the entry β_{ij} encodes the contribution for the allocatalytic cycle



where \mathbf{c}^* denotes a reaction vector for the catalytic cycle, for any description that verifies nonambiguity. When $i = j$, this is a type I autocatalytic cycle (Fig. S6c). When $i \neq j$ (cross-incorporation), type II autocatalytic cycles are obtained, which are built up from n sequential allocatalytic incorporation steps and which end in the incorporation of the original amphiphile. Fig. S6 shows examples for $n = 2$ and $n = 3$. The importance of the allocatalysis step (42) is graded by the entry β_{ij} . For a given n -step autocatalytic motif to exist, we require

$$\prod_{k=1}^n \beta_{s_{k+1}s_k} > 0, \quad s_1 \neq s_2 \neq \dots \neq s_n. \quad (43)$$

In practice, all $\beta_{ij} > 0$, so all motifs exist in principle.

The starting point of GARD is Eq. (39), i.e. a coarse-grained description in which allocatalysis can be described as a single step and a single allocatalyst. From Fig. S6, we see that we can obtain networks in GARD that would be RAF-sets in the RAF-framework by coarse-graining an incorporation cycle to convert it to catalysis in the RAF sense. The illustrated procedure extends to all autocatalysis in GARD, which is fully characterized by the continuation of the structures in Fig. S6 to their n -step type II analogues. Eq. (43) guarantees that each reaction in GARD is catalyzed. It follows that all autocatalysis in the GARD model can formally be treated as a RAF-set.

Interestingly, the RAF-set formalism treats catalysis as pertaining to chemistry in single phases, with the environment supplying food locally through rapid exchange. In GARD, we instead have phase-transfer catalysis between a bulk medium (II) and an interface (I). A species in the bulk then serves as the food. Once the exact same species enters the interface, however, it may cease to be abundant or have a fixed concentration due to rapid exchange. It may thus no longer have the properties ascribed to the food set in the bulk and should ipso facto be treated as a different species as described in the final section of the main text.

V. THE EXTINCTION PROBLEM AND FIXATION

In this section, we show that the extinction problem (finding the extinction probability at long times, P_{ex}) can be solved by a mapping to a branching process. We will first derive how (*context*) in a system initially at steady-state perturbed with dilute autocatalysts, key statistical properties emerge: autocatalytic species can be treated as independent, and their environment as fixed. Extinction becomes exponentially less likely as the population size continues to grow, which means P_{ex} can be determined in the dilute limit.

We then proceed by applying the framework to a variety of networks.

A. Context

We consider a reaction network, in a macroscopic system (Letting N denote the amount of chemical species, let us say $N > 10^{23}$, or similarly, let the system volume V be large) in a steady-state. For simplicity, let us first consider a CSTR (single phase, ideally mixed), with a residence time τ , corresponding to a uniform degradation rate k_d .

Now, we perturb the steady-state with a handful ($O(1)$) of new (not yet present in the system) autocatalysts $\{X_k\} = \{X_1, X_2, \dots, X_s\}$ that are part of the same autocatalytic core.

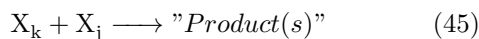
We consider that the population can grow due to catalysis by autocatalysts, and the population decays by degradation reactions and effective degradation. For example, outflow out of a CSTR is considered as a first-order degradation process:



The problem we wish to solve is the extinction problem: For an initial population of autocatalysts $\{N_{X_k}\} = \{N_{X_1}, \dots, N_{X_s}\}$ what is the probability $P_{ex}(\{N_{X_k}\})$, that, after a long time, the autocatalyst population goes extinct ($\forall k \ N_{X_k} = 0$)?

B. Large system limit

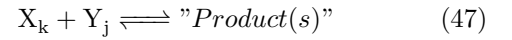
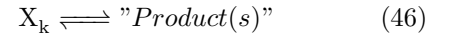
Let us first note that we (deliberately) consider the initial stochastic kinetics in a large system, with a small number of autocatalysts, such that reactions among autocatalysts of the kind



are exceedingly rare and slow (the probability that a given X_k molecule encounters another X_j in a given time-frame scales with N_{X_j}/N), where N_{X_j} is initially

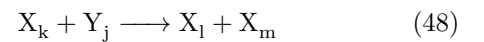
of the order 1. It follows survival of autocatalytic cycles requiring such reactions in the forward sense is hampered in large systems.

Reactions that are first order in terms of autocatalysts are not hampered



where Y_j is a feedstock compound that was already (abundantly) present in the system at a fixed molar fraction x_{Y_j} . The probability for one X_k molecule to encounter a Y_j does not change with N , as x_{Y_j} remains fixed (and macroscopic).

Note furthermore that, when autocatalysts are rare, reactions producing more autocatalysts are 'irreversible'



in the sense that the reverse reaction is exceedingly more rare than the forward reaction.

C. Constant composition, constant transition rates

The effect of rare autocatalysts on the steady-state composition (maintained by influx and degradation in a CSTR) is initially small: every reaction introduces changes in molar fraction of the order $1/N$ (or in concentration terms, $1/V \propto 1/N$). For large N , the alterations of the composition will be vanishingly small while the autocatalysts are rare.

Consequently, we can approximate the reactor composition in which an autocatalyst is placed, as the steady-state composition before perturbation. We then assume that the molar fractions of species Y_k consumed by autocatalysts are sufficiently abundant i.e. $x_{Y_k} \gg 1/N$, which was also required for (47). For sufficient N , deviations from this approximation become vanishingly small.

A given X_k will therefore have a fixed transition rate $w_k^+ = kx_{Y_j}$ to perform (47). Similarly, for (46) and CSTR degradation, a fixed transition rate $w = k$ is found, depending only on a rate constant.

D. Independence

In the rare-autocatalyst regime, all reaction steps we consider for autocatalysts are first-order, and they occur at fixed rates. It follows that autocatalysts do not influence each other, and they can each be treated independently. Thus, we can treat each autocatalyst type separately:

$$P_{ex}(\{N_{X_k}\}) = P_{ex}(N_{X_1})P_{ex}(N_{X_2})\dots P_{ex}(N_{X_s}). \quad (49)$$

Also each individual autocatalyst can be treated as such:

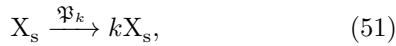
$$P_{ex}(N_{X_k}) = P_{ex}(X_k)^{N_{X_k}} \quad (50)$$

Where $P_{ex}(X_k)$ denotes the extinction probability of a population initially composed of a single X_k species.

We thus need a method for finding $P_{ex}(X_k)$. This will be obtained by mapping the problem to a branching process.

E. A branching process

An attractive method we propose for finding $P_{ex}(X_k)$ (from here on simplified to P_{ex}), is by considering the distribution of 'descendants' X_k a species X_k will generate. From this, we construct a Branching Process, represented chemically as a single parent molecule X_s yielding k descendants:



with \mathfrak{P}_k a distribution of the number of descendants which depends on the network topology.

Knowing \mathfrak{P}_k suffices to find P_{ex} , since the probability to go extinct is the probability that all descendants independently (Eq. (50)) go extinct:

$$P_{ex} = \mathfrak{P}_0 + \mathfrak{P}_1 P_{ex} + \mathfrak{P}_2 P_{ex}^2 + \dots = \sum_{k=0}^{\infty} \mathfrak{P}_k P_{ex}^k, \quad (52)$$

We will now highlight some possible choices for Branching Processes and their associated \mathfrak{P}_k .

F. A Birth-Death Process for the Type I cycle

Consider a simple type-I cycle such as in Fig S7a. Here, simple refers to there being a direct path of (effective) unimolecular steps between the starting compound (B_1) and final compound (B_2), followed by a single fragmentation step producing two B_1 from one B_2

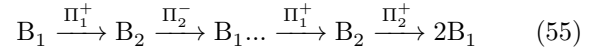


Starting from the marked node (B_1), let $\mathfrak{P}_2 = p_c$ be the probability of successfully forming $2B_1$, i.e.

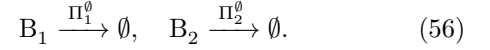


where p_c contains the contribution of all possible trajectories (here: going back and forth between B_1 and B_2) that precede the irreversible fragmentation step,

i.e.



Where Π_1^+ , Π_2^- and Π_2^+ are success probabilities for the single reaction steps. These transitions compete with irreversible degradation processes

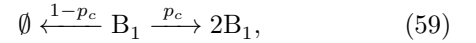


Where Π_1^0 , Π_2^0 are success probabilities for the degradation reaction. Due to total probability conservation, we have

$$\Pi_1^0 + \Pi_1^+ = 1, \quad (57)$$

$$\Pi_2^0 + \Pi_2^- + \Pi_2^+ = 1 \quad (58)$$

Ultimately, a B_1 species will either be replaced by 2 new ones ($2B_1$), or none (\emptyset):



which is a chemical representation of the simplest type of branching process: a birth-death process. In Eq. (52), the only nonzero terms will come from 0 descendants (\mathfrak{P}_0) and 2 descendants (\mathfrak{P}_2):

$$P_{ex} = \mathfrak{P}_0 + \mathfrak{P}_2 P_{ex}^2 = 1 - p_c + p_c P_{ex}^2. \quad (60)$$

Solving the quadratic equation yields two solutions

$$P_{ex}^{\pm} = \frac{1 \pm (1 - 2p_c)}{2p_c}. \quad (61)$$

For our problem, the 'physical' solution is P_{ex}^+ while $p_c \geq 1/2$. Beyond that point, $P_{ex}^+ > 1$, while we require $0 \leq P_{ex} \leq 1$, so $P_{ex}^- = 1$ becomes the only physical solution.

$$P_{ex} = \begin{cases} \frac{1}{p_c} - 1, & p_c \geq \frac{1}{2}, \\ 1, & p_c < \frac{1}{2}, \end{cases} \quad (62)$$

The average number of descendants is $2p_c$, which means that below $p_c = 1/2$ (the decay threshold) B_1 is on average replaced by less than one B_1 species and extinction is guaranteed.

G. A Branching Process for the same type I cycle

To illustrate that there is a variety of choices for the stochastic process under study, we will here consider an alternative choice for the simple type-I cycle, which is more generally applicable. Noting that a single cycle is successful with probability p_c , we now consider the number of successful cycles a single B_1 provides, knowing that at some point degradation intervenes with probability $1 - p_c$. A succession of k cycles preceding

a failure will thus lead to k successors



The probability to spawn k descendants, \mathfrak{P}_k , is the probability of k successful Bernoulli trials followed by failure, and follows a geometric distribution

$$\mathfrak{P}_k = p_c^k (1 - p_c). \quad (64)$$

Injecting this distribution in Eq. (52), we find a geometric series

$$P_{ex} = \sum_{k=0}^{\infty} (1 - p_c) (p_c P_{ex})^k = \frac{1 - p_c}{1 - p_c P_{ex}}. \quad (65)$$

Multiplying both sides by $1 - p_c P_{ex}$ then yields the quadratic equation (60) previously found for the Birth-Death process. This is necessary, since we are calculating the same quantity P_{ex} for the same network. It highlights that we may construct a variety of branching processes to find P_{ex} .

H. A microscopic view on p_c

We can construct p_c from microscopic details. In terms of transition probabilities, we find p_c by summing over all trajectories in Eq.(55):

$$p_c = \sum_{k=0}^{\infty} \Pi_1^+ (\Pi_2^- \Pi_1^+)^k \Pi_2^+ = \frac{\Pi_1^+ \Pi_2^+}{1 - \Pi_2^- \Pi_1^+} \quad (66)$$

A more detailed description is possible when our description is Markovian (i.e. reactions are sufficiently elementary). Let w_k^+ denote a forward transition rate, to go from X_k to X_{k+1} . Let w_k^- denote a backward transition rate from X_k to X_{k-1} and w_k^\emptyset the degradation rate for X_k . We may then write

$$\Pi_1^+ = \frac{w_1^+}{w_1^+ + w_1^\emptyset}, \quad \Pi_2^- = \frac{w_1^-}{w_1^- + w_2^\emptyset + w_2^+}, \quad (67)$$

$$\Pi_2^+ = \frac{w_2^+}{w_1^- + w_2^\emptyset + w_2^+}. \quad (68)$$

I. The irreversible reaction limit

Simple type-I cycles have been studied on several occasions, in the limit where all reactions proceed irreversibly^{21,23,45} ($\forall k \ w_k^- \rightarrow 0$). In this limit backward reactions are ignored ($\Pi_2^- = 0$), which for our example leads to

$$p_c = \Pi_1^+ \Pi_2^+ = \frac{w_1^+}{w_1^+ + w_1^\emptyset} \frac{w_2^+}{w_2^+ + w_2^\emptyset}. \quad (69)$$

In this limit, there is only one trajectory that contributes to p_c , and each step involves a competition between the forward reaction and degradation only.

In studies using simple type-I cycles, the fraction

$$\zeta_k = \frac{w_k^+}{w_k^+ + w_k^\emptyset}, \quad (70)$$

has been referred to as the specificity of reaction step^{23,44,45,58} k , which for irreversible reactions coincides with the transition probability Π_k^+

$$\lim_{w_{k-1}^- \rightarrow 0} \Pi_k^+ = \lim_{w_{k-1}^- \rightarrow 0} \frac{w_k^+}{w_{k-1}^- + w_k^+ + w_k^\emptyset} = \zeta_k \quad (71)$$

For simple type-I networks with n reaction steps (n distinct edges), the irreversible limit (Eq. (69)) generalizes to^{44,58}

$$p_c = \prod_{k=1}^n \Pi_k^+ = \prod_{k=1}^n \frac{w_k^+}{w_k^+ + w_k^\emptyset}, \quad (72)$$

which we will show more formally in the next section.

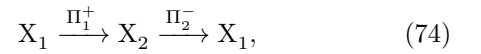
J. The simple type I cycle with n steps

To expand our discussion on simple type I cycles, we will now derive a general expression for p_c , when there are n steps, of which the first $n - 1$ are treated as reversible. The problem is illustrated in Fig. S7c.

Let us denote $P_{X_k \rightarrow X_j}$ the probability to reach X_j , starting from X_k . For $P_{X_1 \rightarrow X_2}$, there is only one trajectory:



and hence $P_{X_1 \rightarrow X_2} = \Pi_1^+$. For $P_{X_2 \rightarrow X_3}$, we need to consider that we can go back and forth between X_2 and X_1 :



We can absorb the contribution of hopping back-and-forth in the factor Γ_2 :

$$P_{X_2 \rightarrow X_3} = \Pi_2^+ \Gamma_2 \quad (76)$$

$$\Gamma_2 = \sum_{k=0}^{\infty} (\Pi_2^- \Pi_1^+)^k = \frac{1}{1 - \Pi_2^- \Pi_1^+} \quad (77)$$

Now, for $P_{X_3 \rightarrow X_4}$, we need to consider that we can go back and forth between X_3 and X_2 , and that at X_2 we can go back and forth between X_2 and X_1 . We absorb

this in the factor Γ_3 :

$$P_{X_3 \rightarrow X_4} = \Pi_3^+ \Gamma_3 \quad (78)$$

$$\Gamma_3 = \sum_{k=0}^{\infty} (\Pi_3^- \Gamma_2 \Pi_2^+)^k = \frac{1}{1 - \Pi_3^- \Gamma_2 \Pi_2^+} \quad (79)$$

We can repeat this argument any number of times, to find that, for $k \geq 1$

$$P_{X_k \rightarrow X_{k+1}} = \Pi_k^+ \Gamma_k \quad (80)$$

$$\Gamma_{k+1} = \sum_{s=0}^{\infty} (\Pi_{k+1}^- \Gamma_k \Pi_k^+)^s = \frac{1}{1 - \Pi_{k+1}^- \Gamma_k \Pi_k^+}. \quad (81)$$

where Γ_2 imposes that $\Gamma_1 = 1$.

The total probability p_c to reach X_n from X_1 and then perform the final irreversible fragmentation reaction r_n , is then

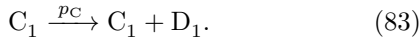
$$p_c = \left(\prod_{k=1}^{n-1} P_{X_k \rightarrow X_{k+1}} \right) \Pi_n^+ \Gamma_n = \prod_{k=1}^n \Pi_k^+ \Gamma_k, \quad (82)$$

When backward transitions become negligible ($\forall k \Pi_k^- \rightarrow 0$), we have $\forall k \geq 1 \Gamma_k = 1$, and p_c then acquires its well-known limit expression described by Eq. (72).

K. A Branching Process for a Type II cycle

As an example of a simple type-II cycle, we consider the network in Fig. S7c, starting with the species C_1 . Our approach will be reminiscent of our branching process in Sec. V G, but with a repeated branching step.

With a probability p_C , C_1 will successfully perform the allocatalytic cycle $r_1 + r_2 + r_3$ (with some possible back-and-forths), yielding overall



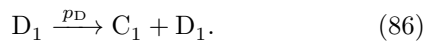
The probability \mathcal{P}_k^D that k successful cycles occur before the first failure (i.e. degradation $C_k \rightarrow \emptyset$) is

$$\mathcal{P}_k^D = (1 - p_C) p_C^k. \quad (84)$$

Corresponding effectively to the overal reaction



Now, let p_D be the probability that D_1 successfully completes a cycle $r_4 + r_2 + r_3$ (including back-and-forths):



The probability of k successful cycles before failure

becomes

$$\mathcal{P}_k^C = (1 - p_D) p_D^k. \quad (87)$$

Combined, a single C_1 has been then replaced according to

$$C_1 \longrightarrow s D_1 \longrightarrow (n_1 + n_2 + \dots + n_s) C_1. \quad (88)$$

Let us denote $k = \sum_{l=1}^s n_l$ as the number of descendants. The distribution of the number of descendants \mathfrak{P}_k then becomes

$$\mathfrak{P}_k = \sum_{s=0}^{\infty} \mathcal{P}_s^P \sum_{n_1, \dots, n_s} \prod_{r=0}^s \mathcal{P}_{n_r}^{\text{DCU}} \delta_{n_1 + \dots + n_s}^k, \quad (89)$$

which simplifies to

$$\mathfrak{P}_0 = 1 - \beta \frac{\alpha}{1 - \alpha}, \quad \mathfrak{P}_k = \beta \alpha^k, \quad k \geq 1 \quad (90)$$

where

$$\alpha = \frac{p_D}{1 - p_C(1 - p_D)}, \quad \beta = \frac{p_C(1 - p_D)(1 - p_C)}{1 - p_C(1 - p_D)}. \quad (91)$$

From Eq. (52), we then find P_{ex} . By rewriting the geometric series due to (91), we have

$$P_{ex} = 1 - \beta \frac{\alpha}{1 - \alpha} - \beta \frac{\alpha P_{ex}}{1 - \alpha P_{ex}}, \quad (92)$$

which admits the solutions $P_{ex} = 1$ and

$$P_{ex} = \frac{\beta}{\alpha - 1} + \frac{1}{\alpha} = \frac{1 - p_C}{p_D}. \quad (93)$$

L. Microscopic expressions for p_C and p_D

Let us first consider how p_C can be constructed from smaller reaction steps. To do so, we observe that the first step must be



with Π_1^+ the probability of success, competing with degradation



for which $\Pi_1^0 = 1 - \Pi_1^+$.

Arrived at C_2 , going back-and forth reversibly

becomes possible for neighboring nodes C_1 , C_3 and D_1 :

$$C_1 \xrightarrow{\Pi_1^+} C_2, \quad C_2 \xrightarrow{\Pi_2^-} C_1 \quad (96)$$

$$C_2 \xrightarrow{\Pi_2^+} C_3, \quad C_3 \xrightarrow{\Pi_3^-} C_2 \quad (97)$$

$$C_2 \xrightarrow{\Theta_1^-} D_1, \quad D_1 \xrightarrow{\Theta_1^+} C_1 \quad (98)$$

Where Π_k^+ , Π_k^- , Θ_k^- , Θ_k^+ all denote success probabilities. Starting at C_1 , a succesful trajectory necessarily starts with reaction r_1 (Π_1^+) and ends with $r_2 + r_3$ ($\Pi_2^+ \Pi_3^+$), all in the forward sense. In between, we can go back-and-forth ($\Pi_2^- \Pi_1^+ + \Theta_2^- \Theta_1^+ + \Pi_2^+ \Pi_3^-$) any number of times. Summing over all possible trajectories, p_C then becomes

$$p_C = \sum_{k=0}^{\infty} \Pi_1^+ (\Pi_2^- \Pi_1^+ + \Theta_2^- \Theta_1^+ + \Pi_2^+ \Pi_3^-)^k \Pi_2^+ \Pi_3^+ \quad (99)$$

which sums to

$$p_C = \frac{\Pi_1^+ \Pi_2^+ \Pi_3^+}{1 - (\Pi_2^- \Pi_1^+ + \Theta_2^- \Theta_1^+ + \Pi_2^+ \Pi_3^-)} \quad (100)$$

Starting at D_1 , a succesful trajectory necessarily starts with r_4 (Θ_1^+) in the forward sense, to form C_2 . From there on, a successful trajectory follows the previous calculation, i.e. $p_D = (\Theta_1^+ / \Pi_1^+) p_C$:

$$p_D = \frac{\Theta_1^+ \Pi_2^+ \Pi_3^+}{1 - (\Pi_2^- \Pi_1^+ + \Theta_2^- \Theta_1^+ + \Pi_2^+ \Pi_3^-)} \quad (101)$$

In the limit where all reactions proceed irreversibly forward (Sec. VI), p_C and p_D only have a contributing from a single straight trajectory

$$p_C = \Pi_1^+ \Pi_2^+ \Pi_3^+, \quad p_D = \Theta_1^+ \Pi_2^+ \Pi_3^+. \quad (102)$$

M. Type III cycles with one fragmentation step

Let us now consider a type III network composed of n species $\{X_1, \dots, X_n\}$ and reaction steps $\{r_1, \dots, r_n\}$, where the final fragmentation step r_n produces

$$X_n \longrightarrow X_1 + X_s, \quad 1 < s < n, \quad (103)$$

as shown in Fig. S7e

We may then introduce the success rates for the allocatalytic cycles for X_1 and X_s

$$X_1 \xrightarrow{p_1} X_1 + X_s, \quad (104)$$

$$X_s \xrightarrow{p_s} X_1 + X_s. \quad (105)$$

Which was exactly our starting point in Sec. VK. Starting at X_s , we may thus directly use P_{ex} , upon

replacing p_C with p_s and p_D with p_1 , thus finding

$$P_{ex} = \frac{1 - p_s}{p_1}. \quad (106)$$

We now turn to the problem of finding expressions for p_s and p_1 .

By structural analogy to simple type I cycles (apart from the fragmentation step), we may again write

$$P_{X_k \rightarrow X_{k+1}} = \Pi_k^+ \Gamma_k \quad (107)$$

$$\Gamma_{k+1} = \sum_{s=0}^{\infty} (\Pi_k^- \Gamma_k \Pi_k^+)^s = \frac{1}{1 - \Pi_{k+1}^- \Gamma_k \Pi_k^+}. \quad (108)$$

with $\Gamma_1 = 1$.

Since $p_s = \left(\prod_{k=s}^{n-1} P_{X_k \rightarrow X_{k+1}} \right) \Pi_n^+ \Gamma_n$ we find

$$p_s = \left(\prod_{k=s}^n \Pi_k^+ \Gamma_k \right) \quad (109)$$

N. Symmetric motifs

When the network motif is symmetric in structure, and if the transitions preserve this symmetry, this can be exploited to simplify calculations and gain insight in topological aspects of autocatalysis and robustness. Experimentally, this symmetry rarely applies for the transitions, but it can be made applicable for the purpose of our analysis, e.g. by setting transition probabilities to values that reflect the structural symmetry.

Consider a series of m linked allocatalytic cycles (Fig. S8b), all consisting of n nodes and n edges which are structurally equivalent:

$$X_{kn+1} \xrightarrow{\Pi_{kn+1}^+} \dots \xrightarrow{\Pi_{(k+1)n}^+} X_{kn+1} + X_{(k+1)n+1}, \quad (110)$$

which loops back at the m th cycle:

$$X_{m-n+1} \xrightarrow{\Pi_{m-n+1}^+} \dots \xrightarrow{\Pi_{mn}^+} X_1 + X_{m-n+1}, \quad (111)$$

As before, Π_k^+ denotes a forward transition probability, and we also introduce reverse reactions and degradation in the usual sense:

$$X_k \xrightarrow{\Pi_k^-} X_{k-1}, \quad (112)$$

$$X_k \xrightarrow{\Pi_k^\emptyset} \emptyset. \quad (113)$$

Now, let us choose transition probabilities such that they are equivalent among the equistructural allocatalytic cycles, i.e. periodic in n : $\Pi_k^+ = \Pi_{k+n}^+$ and idem for reverse steps ($\Pi_k^- = \Pi_{k+n}^-$) and by extension, degradation ($\Pi_k^\emptyset = \Pi_{k+n}^\emptyset$), since $\Pi_k^+ + \Pi_k^- + \Pi_k^\emptyset = 1$.

Then, finding $P_{ex}(X_k)$ is no different⁵⁹ from finding $P_{ex}(X_{k+n})$, which is seen readily in Fig. S8a by rotating the networks and interchanging the labels. Applying this symmetry to Fig.S8a for the six-membered cycle ($n = 2, m = 3$), we can thus write

$$\begin{aligned} P_{ex}(X_1) &= P_{ex}(X_3) = P_{ex}(X_5). \\ P_{ex}(X_2) &= P_{ex}(X_4) = P_{ex}(X_6). \end{aligned} \quad (114)$$

We characterize the success of each equivalent allocatalytic cycle (n steps) by the same probability p_c . We can then express the extinction probability in terms of the reaction products of one allocatalytic cycle:

$$\begin{aligned} P_{ex}(X_1) &= 1 - p_c + p_c P_{ex}(X_1) P_{ex}(X_3) \\ &= 1 - p_c + p_c P_{ex}(X_1)^2, \end{aligned} \quad (115) \quad (116)$$

where we have used the symmetry (115), which yields the exact second order equation we obtained for a simple type-I cycle of n steps. We can thus resolve the general problem using our previously derived solutions.

VI. EXPRESSIONS FOR FIG 3, A SURVEY OF P_{ex} FOR VARIOUS STRUCTURES

In Fig. 3 in the main text, the behavior of P_{ex} is compared for a number of networks (N_1 to N_5), in the limit where all reaction steps proceed irreversibly (Sec. VI), and where all reaction steps do so with a common success probability ζ (also known in the literature as specificity). Of course, this is an abstraction that is hard to realize experimentally, and its purpose is the following: by controlling for kinetics, we can systematically investigate and compare how survival is affected by network topology. In this section, we will derive the functional dependence of P_{ex} on ζ for the structures discussed in the main text.

1. N_1 : a 6-membered type I cycle

In Sec. V J, we derived the general solution for n -membered type I cycles in terms of the probability p_c to reach X_n and perform r_n . Starting from X_1 , we can now recover the solution for $n = 6$

For $n = 6$, p_c becomes

$$p_c = \left(\prod_{k=1}^5 P_{X_k \rightarrow X_{k+1}} \right) \Pi_6^+ \Gamma_6 = \prod_{k=1}^6 \Pi_k^+ \Gamma_k \quad (117)$$

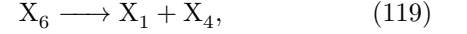
Moving to the irreversible reaction limit, and controlling the reaction specificity ($\forall k \geq 1 \Pi_k^+ = \zeta, \Gamma_k = 1$), we obtain $p_c = \zeta^6$. Upon injection in the solution $P_{ex} = (1 - p_c)/p_c$ (for $p_c \geq 1/2$) (Eq. (9)), we then

find

$$P_{ex} = \frac{1 - \zeta^6}{\zeta^6} \quad (118)$$

2. N_2 : a 6-membered asymmetric type III cycle

In Sec. V M, the general solution for n -membered type III cycles with one fragmentation reaction was derived. For a 6-membered cycle with the fragmentation reaction



which corresponds to network N_2 in the main text.

Having X_4 as the starting species, we can express $P_{ex}(X_4)$ in terms of Eq. (109)

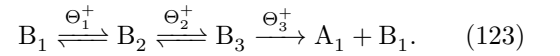
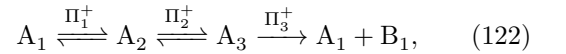
$$P_{ex} = \frac{1 - p_4}{p_1}. \quad (120)$$

In the irreversible reaction limit with fixed specificity ($\forall k \geq 1 \Pi_k^+ = \zeta, \Gamma_k = 1$), P_{ex} becomes

$$P_{ex} = \frac{1 - \zeta^3}{\zeta^6} \quad (121)$$

A. N_3 : 6-membered type II network with RAF representation

The network N_3 consists of two nonoverlapping allocatalytic cycles, which produce each other's allocatalyst:



Choosing our transition probabilities $\Pi_k^+ = \Theta_k^+$, we can exploit the network symmetry as outlined in Sec. V N and $P_{ex}(A_1) = P_{ex}(B_1)$. Let p_c be the probability that either A_1 or B_1 successfully finishes an allocatalytic cycle. We may then write

$$P_{ex}(A_1) = 1 - p_c + p_c P_{ex}(A_1) P_{ex}(B_1) \quad (124)$$

$$= 1 - p_c + p_c P_{ex}(A_1)^2. \quad (125)$$

The success rate p_c can be expressed in the familiar way

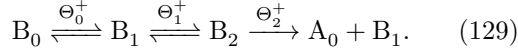
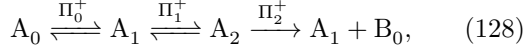
$$p_c = \Pi_1^+ \Pi_2^+ \Pi_3^+ \Gamma_1 \Gamma_2 \Gamma_3. \quad (126)$$

In the irreversible limit ($\forall k \geq 1, \Gamma_k = 1$) with fixed specificity ζ , $p_c = \zeta^3$, and thus we find for $p_c \geq 1/2$

$$P_{ex} = \frac{1 - \zeta^3}{\zeta^3}. \quad (127)$$

B. N_4 : 6-membered symmetric type III network

The network N_4 consists of two nonoverlapping allocatalytic cycles, which produce a precursor (A_0, B_0) for each other's allocatalyst:



Choosing our transition probabilities to follow the symmetry of the network, we can write $\Pi_k^+ = \Theta_k^+$, and $P_{ex}(A_k) = P_{ex}(B_k)$. Finally, we note that B_0 can either i) degrade with probability $\Theta_0^\emptyset = 1 - \Theta_0^+$, or ii) form B_1 with probability $\Theta_0^+ = \Pi_0^+$, such that

$$P_{ex}(B_0) = 1 - \Pi_0^+ + \Pi_0^+ P_{ex}(B_1) = 1 - \Pi_0^+ + \Pi_0^+ P_{ex}(A_1). \quad (130)$$

Denoting p_c the probability that A_1 performs a successful allocatalytic cycle (yielding $A_1 + B_0$), we can write the extinction probability as

$$P_{ex}(A_1) = 1 - p_c + p_c P_{ex}(A_1) P_{ex}(B_0), \quad (131)$$

which upon injecting (130) yields the following expression for $P_{ex}(A_1)$

$$P_{ex} = 1 - p_c + p_c(1 - \Pi_0^+) P_{ex} + p_c \Pi_0^+ P_{ex}^2. \quad (132)$$

Solving the quadratic equation (132), we find

$$P_{ex}(A_1) = \frac{1 - p_c(1 - \Pi_0^+) \pm \sqrt{(p_c(1 - \Pi_0^+) - 1)^2}}{2p_c \Pi_0^+} \quad (133)$$

which yields $P_{ex} = 1$ and

$$P_{ex} = \frac{1 - p_c}{p_c \Pi_0^+}. \quad (134)$$

We can write p_c in terms of back-and-forths starting at A_1 , terminating with an irreversible fragmentation

$$p_c = \sum_{k=0}^{\infty} (\Pi_1^- \Pi_0^+ + \Pi_1^+ \Pi_2^-)^k \Pi_1^+ \Pi_2^+ \quad (135)$$

$$= \frac{\Pi_1^+ \Pi_2^+}{1 - \Pi_1^- \Pi_0^+ + \Pi_1^+ \Pi_2^-}, \quad (136)$$

so that in the irreversible limit with fixed specificity ($\forall k \geq 1, \Pi_{k+} = \zeta, \Pi_{k-} = 0$), we obtain

$$P_{ex} = \frac{1 - \zeta^2}{\zeta^3}. \quad (137)$$

An alternative way of seeing this is that, by symmetry, P_{ex} is the same as that for a 3-membered type III cycle with one fragmentation step (forming X_2), for which we can directly use the solution derived in Sec. VM.

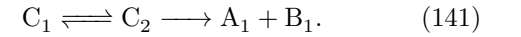
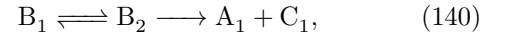
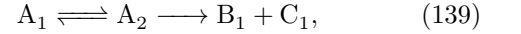
C. A trio of symmetric analogues

As derived in Sec. VN, the interlinked allocatalytic cycles of size n behave, due to symmetry, as an n -membered simple type-I cycle. Reproducing the solution for the 2-membered cycles (see Sec. VF) in the irreversible limit with $\forall k \geq 1, \Pi_k^+ = \zeta, \Pi_k^- = 0$, we thus find

$$P_{ex} = \frac{1 - \zeta^2}{\zeta^2} \quad (138)$$

D. N_5 : a type V core

In N_5 we have the reactions



If our transitions follow the symmetry of the network, we have $P_{ex}(A_k) = P_{ex}(B_k) = P_{ex}(C_k)$. Denoting p_c the success probability of the allocatalytic cycle, we can write P_{ex} in terms of Eq. (139)

$$P_{ex}(A_1) = 1 - p_c + p_c P_{ex}(B_1) P_{ex}(C_1) \quad (142)$$

$$= 1 - p_c + p_c P_{ex}(A_1)^2, \quad (143)$$

which is the solution found for the 2-membered cycle. Noting that

$$p_c = \Pi_1^+ \Pi_2^+ \Gamma_1 \Gamma_2 \quad (144)$$

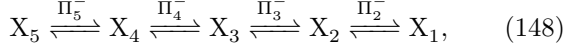
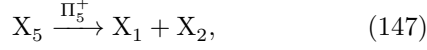
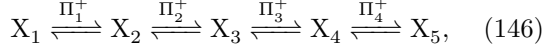
the irreversible limit with fixed specificity ($\forall k \geq 1, \Pi_k^+ = \zeta, \Gamma_k = 1$) yields, as in Sec. VF,

$$P_{ex} = \frac{1 - \zeta^2}{\zeta^2} \quad (145)$$

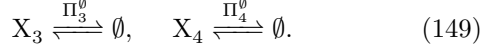
VII. EXPRESSIONS FOR FIG 4D, A PHASE DIAGRAM FOR MULTICOMPARTMENT AUTOCATALYSIS

Fig. S9 represents a case of a type III core with one fragmentation reaction (Sec. VM), consisting of 5

members:



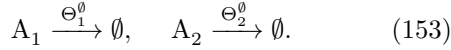
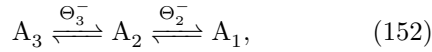
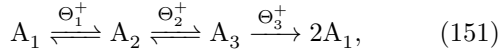
which can also be seen in Fig. S9c. From Fig. S9a, we furthermore infer that there are only two degradation reactions (r_6 and r_7):



Denoting p_1 the probability for X_1 to successfully finish (with back-and-forths) the cycle $r_1 + r_2 + r_3 + r_4 + r_5$, and p_2 the probability that X_2 does so for $r_2 + r_3 + r_4 + r_5$, we can directly substitute the expressions derived in sec. V J

$$p_1 = \prod_{k=1}^5 \Pi_k^+ \Gamma_k, \quad p_2 = \prod_{k=2}^5 \Pi_k^+ \Gamma_k. \quad (150)$$

Since degradation reactions do not occur in compartment I, we are guaranteed that, starting from X_1 or X_2 , eventually X_3 will be formed with probability 1. At that point, we can solve the problem for an effective network without X_1 and X_2 starting at X_3 (by the same token, returns are inconsequential). In Fig. S9d this effective network is given, for which we write



We readily find that this corresponds to a simple type-I network with 3 members, with a success probability for a cycle p_c , such that

$$p_c = \Theta_1^+ \Theta_2^+ \Theta_3^+ \Phi_1 \Phi_2 \Phi_3 \quad (154)$$

$$P_{ex} = \frac{1 - p_c}{p_c} \quad (155)$$

Where we have used Φ_k for calculating back-and-forth trajectories, as derived in sec. V J:

$$P_{A_k \rightarrow A_{k+1}} = \Theta_k^+ \Phi_k \quad (156)$$

$$\Phi_{k+1} = \sum_{s=0}^{\infty} (\Theta_k^- \Phi_k \Theta_k^+)^s = \frac{1}{1 - \Theta_{k+1}^- \Phi_k \Theta_k^+}. \quad (157)$$

with $\Phi_1 = 1$. Let us now give a microscopic interpretation to the competing processes, by considering sufficiently elementary transitions on the level of a single species

- $w_3^+ = k_3^+ x_F$, sequestration of F (see S9a), which

plays the role of a feedstock species in compartment I when r_3 proceeds forward. proceeds backward.

- $w_3^0 = k_3^0$ degradation, r_6
- $w_4^- = k_4^-$ release of F, when r_3
- $w_4^+ = k_4^{ex}$ exchange, from compartment II to I, when r_4 proceeds forward.
- $w_4^0 = k_4^0$ degradation, r_7
- $w_5^- = k_5^{ex}$ exchange, from compartment I to II, when r_4 proceeds backward.
- $w_5^+ = k_5^+$ release of F, which is an autocatalyst in II, through locally irreversible reaction r_5 .

We then obtain

$$\Theta_1^+ = \frac{w_3^+}{w_3^+ + w_3^0}, \quad \Theta_1^0 = \frac{w_3^0}{w_3^+ + w_3^0}, \quad (158)$$

$$\Theta_2^+ = \frac{w_4^+}{w_4^+ + w_4^0 + w_4^-}, \quad \Theta_2^0 = \frac{w_4^0}{w_4^+ + w_4^0 + w_4^-}, \quad (159)$$

$$\Theta_2^- = \frac{w_4^-}{w_4^+ + w_4^0 + w_4^-}, \quad \Theta_3^+ = \frac{w_5^+}{w_5^+ + w_5^-}, \quad (160)$$

$$\Theta_3^- = \frac{w_5^-}{w_5^+ + w_5^-}. \quad (161)$$

Noting that $\Phi_1 = 1$, the product $\Phi_2 \Phi_3$ simplifies to

$$\Phi_2 \Phi_3 = \frac{1}{1 - \Theta_2^- \Theta_1^+ - \Theta_3^- \Theta_2^+}. \quad (162)$$

This allows to fully express P_{ex} in terms of 8 microscopic coefficients. Reactions r_1 and r_2 would give 4 more rate constants and two more molar fractions (for chemostatted species). However, their values do not alter P_{ex} as they will always lead to return to A_1 (provided $w_1^+, w_2^+ > 0$, which we naturally assume to be true).

For the purpose of illustration, we will consider the competition between exchange, degradation, and other transitions. To do so, we choose one rate for exchange $k_4^{ex} = k_5^{ex} = k^{ex}$ and one rate for degradation $k_3^d = k_4^d = k^d$. Furthermore, we let the sequestration-release steps be equally probable in compartment II, and match release in I $w_3^+ = w_4^- = w_5^+ = k$. The transition success probabilities can then be expressed in terms of two ratios

$$\Delta = k^d/k, \quad \Xi = k^{ex}/k \quad (163)$$

which upon substitution yield

$$\Theta_1^+ = \frac{1}{1+\Delta}, \quad \Theta_1^d = \frac{\Delta}{1+\Delta}, \quad \Theta_2^+ = \frac{\Xi}{1+\Delta+\Xi}, \quad (164)$$

$$\Theta_2^d = \frac{\Delta}{1+\Delta+\Xi}, \quad \Theta_2^- = \frac{1}{1+\Delta+\Xi}, \quad (165)$$

$$\Theta_3^+ = \frac{1}{1+\Xi}, \quad \Theta_3^- = \frac{\Xi}{1+\Xi}. \quad (166)$$

This permits to construct the phase diagram for P_{ex} in Fig. 4D in terms of the variables Δ and Ξ .

A. Phase boundaries and limits

Let us first find an expression for the boundary between autocatalysis and deterministic extinction, which occurs when $P_{ex} = 1$ and Eq. (155) coincide, i.e. when $p_c = 1/2$, which upon substitution of Eq. (162) becomes:

$$\Theta_1^+ \Theta_2^+ \Theta_3^+ = \frac{1}{2} (1 - \Theta_2^- \Theta_1^+ - \Theta_3^- \Theta_2^+) \quad (167)$$

In terms of Ξ and Δ , we have

$$2 \frac{1}{1+\Delta} \frac{\Xi}{1+\Delta+\Xi} \frac{1}{1+\Xi} = 1 - \frac{1}{1+\Delta+\Xi} \frac{1}{1+\Delta} - \frac{\Xi}{1+\Xi} \frac{\Xi}{1+\Delta+\Xi} \quad (168)$$

Which rearranges to a linear dependence in Ξ

$$\Delta^2 \Xi + \Delta^2 + 3\Delta \Xi + 2\Delta - \Xi = 0, \quad (169)$$

from which we obtain for the phase boundary

$$\Xi = \frac{\Delta(\Delta + 2)}{1 - 3\Delta - \Delta^2}. \quad (170)$$

In the regime where reactions outpace degradation ($\Delta \ll 1$), extinction will be due to rate-limiting exchange ($\Xi \ll 1$). Taking Eq. (170), dividing by Δ and letting $\Delta \rightarrow 0$, the ratio Ξ/Δ tends to

$$\frac{\Xi}{\Delta} = 2, \quad (171)$$

as also seen in the phase diagram. When exchange is very rapid ($\Xi \rightarrow \infty$), it ceases to be rate-limiting, and degradation will only compete with other reactions. This occurs when we let the denominator of Eq. (170) become 0, i.e.

$$1 - 3\Delta - \Delta^2 = 0, \quad (172)$$

which has solutions

$$\Delta^\pm = \frac{-3 \pm \sqrt{21}}{2}, \quad (173)$$

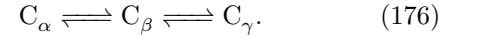
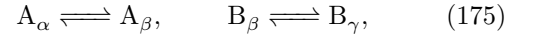
of which $\Delta = \frac{-3+\sqrt{21}}{2} \approx 0.79$ is the physical solution, as can also be seen in the phase diagram.

VIII. MULTICOMPARTMENT AUTOCATALYSIS WITH THREE COMPARTMENTS

Let us consider a bimolecular reaction



which can occur in three different compartments labeled α, β, γ , as shown in Fig. S9d. Let us couple these compartments through the following exchanges



Removing A_γ, C_α then immediately yields the type III autocatalytic core shown in Fig. S9e.

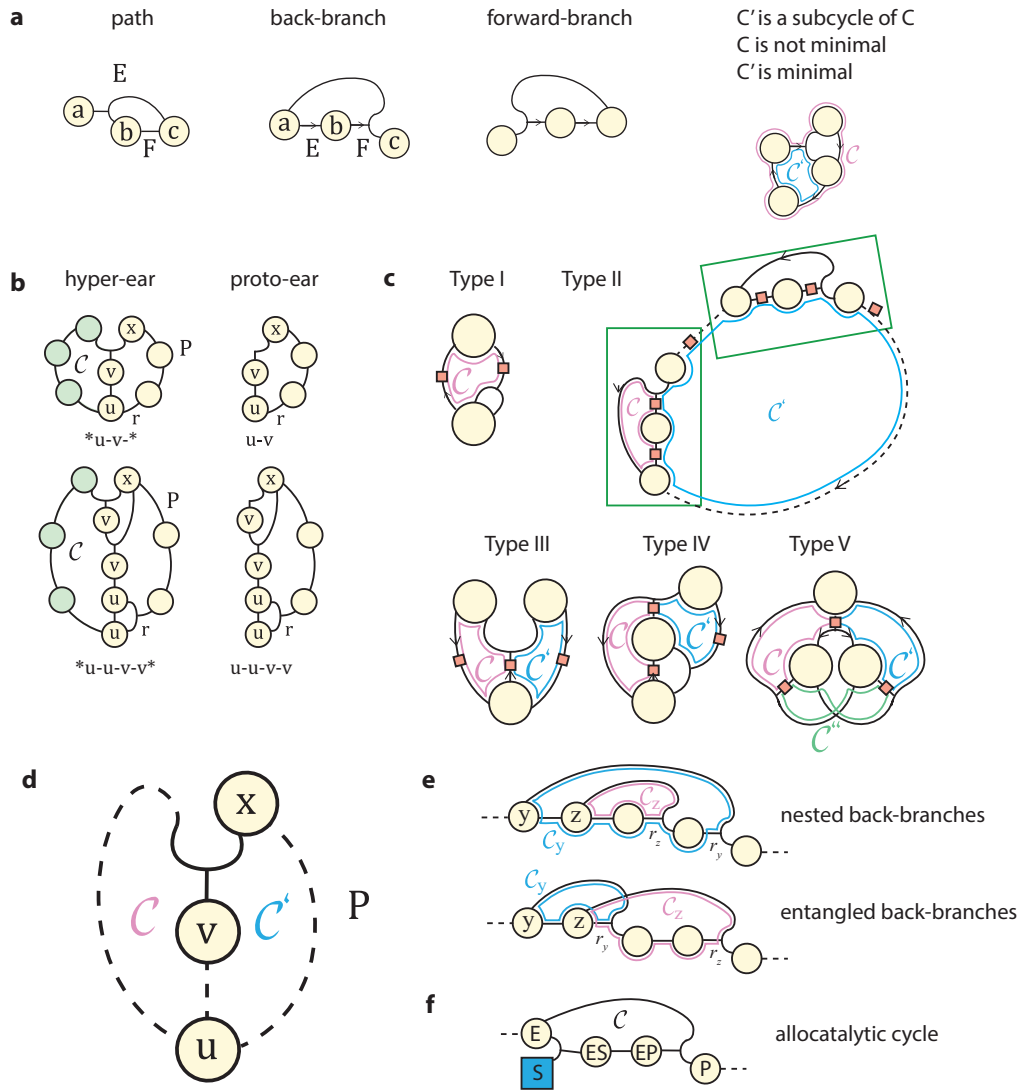


Figure S1: a) Hypergraph paths and cycle examples. b) Examples of hyper-ears (left) and associated proto-ears (right) obtained by removing green species. The syntax below graphs (see section II C) describes the relationships between non-P species and path P. Nodes 'u' are products of r, nodes 'v' are reactants of reactions producing x, '-' is any series of reactions with a single reactant and product, '*' denotes the closure of C by the green path. c) Autocatalytic cores. Edges are oriented consistently along cycles, so that reaction have a single reactant. Orange squares are chains of arbitrary length made of reactions with a single reactant species and product species. Edge-to-node connections are weighted by a stoichiometric coefficient, represented explicitly only for Type I by a fork (stoichiometry of 2). C , C' and C'' are cycles. In Type II, the dotted path may comprise multiple cycles similar to the green box. In main text Fig. 2, only the case of a single green box is represented for simplicity. In Type I, $\det C \neq 0$; in Type II, $\det(C) = 0$ and $\det(C')$ can be any value; in Types III-V, $\det(C) = \det(C') = \det(C'') = 0$. d) Generic hyper-ear structure of cores. e) Nested and entangled back-branches. f) Example of allocatalytic cycle.

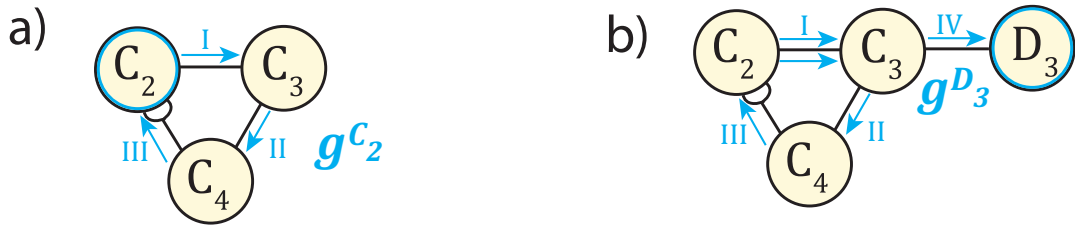


Figure S2: a) A decorated Toy Formose reaction given by the submatrix ν_* , obtained by removing C_1 . The replication cycle g^{D_3} is illustrated in blue. In this network, only species C_2 , C_3 and C_4 are autocatalysts. b) The minimal formose reaction in its autocatalytic subnetwork, an example of an SFA. Arrows illustrate the replication cycle g^{C_2} .

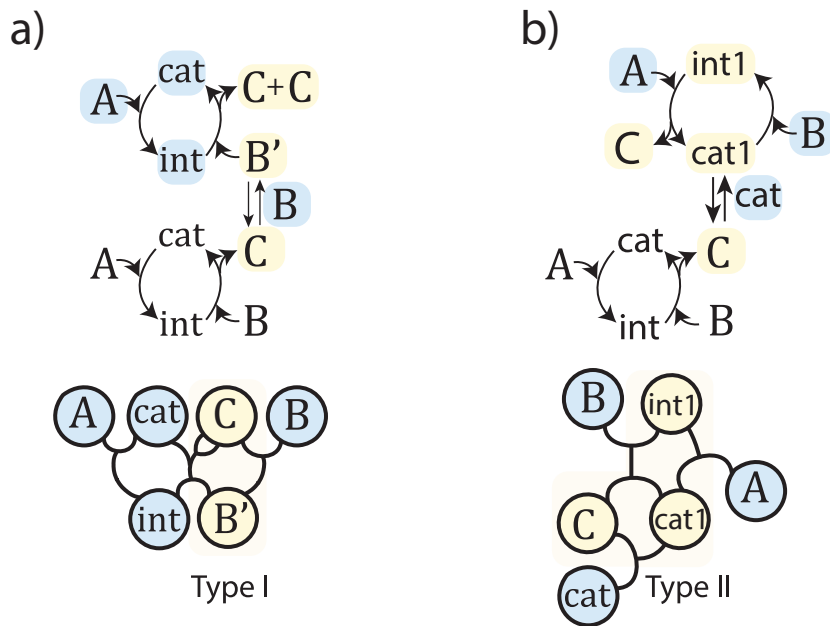


Figure S3: a) top: A product-enhanced cycle, Blackmond's first type of autoinduction. bottom: Hypergraph, containing the type I autocatalytic core (yellow). External food and allocatalysts are marked in blue. b) top: A ligand-accelerated cycle, Blackmond's second type of autoinduction. bottom: Hypergraph, containing the type II autocatalytic core (yellow) and supporting external food (blue). Note that, in both cases, external allocatalytic cycles are not part of the core. Allocatalysts are treated on equal footing with feedstock and waste in isolating a core.

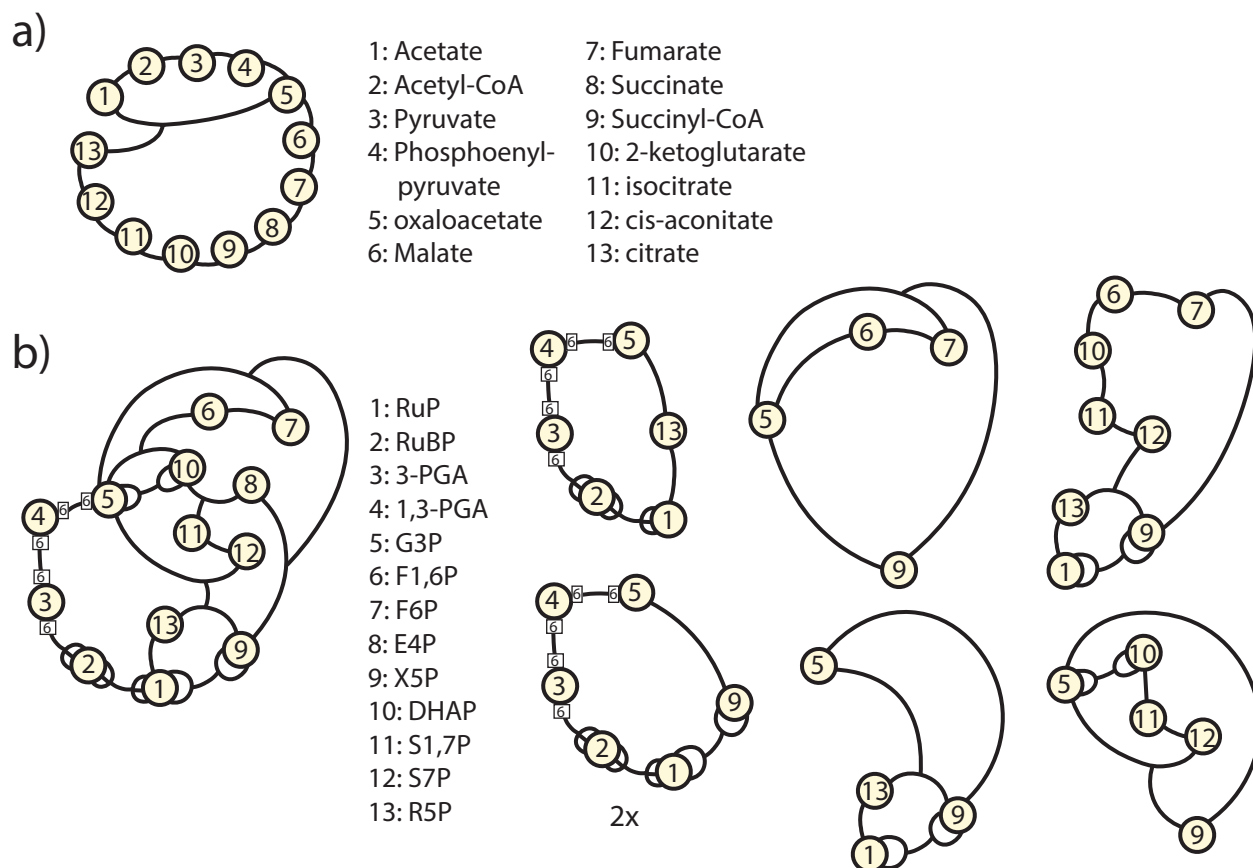


Figure S4: a) Autocatalysts in the Reverse Krebs cycle, which yield a Type II core. b) Autocatalysts in the Calvin Cycle. We find 3 cores of type I (2 equivalent, up to the choice of reaction to link 5 and 9), and 4 cores of type II.

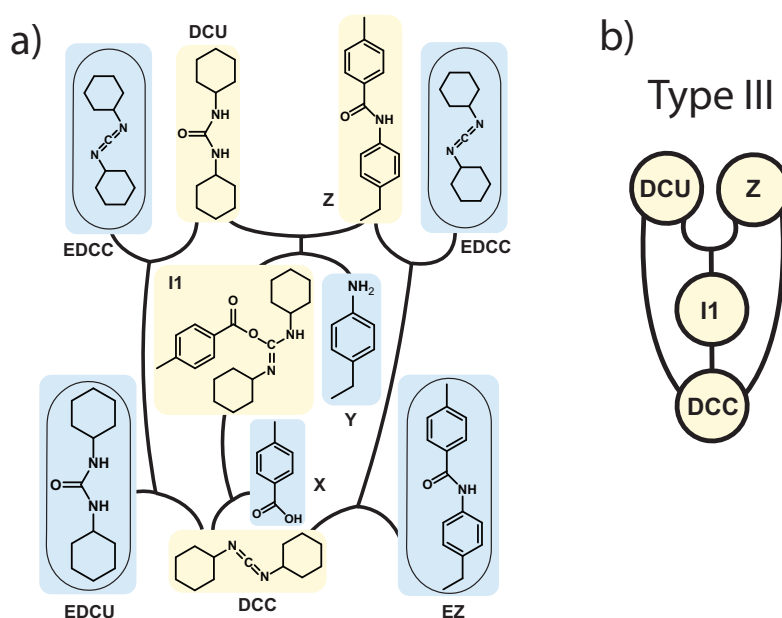


Figure S5: a. Chemical network for the cavitand-amplification network. blue: feedstock compounds and waste. beige: autocatalysts. b. type III autocatalytic core for the cavitand-amplification network.

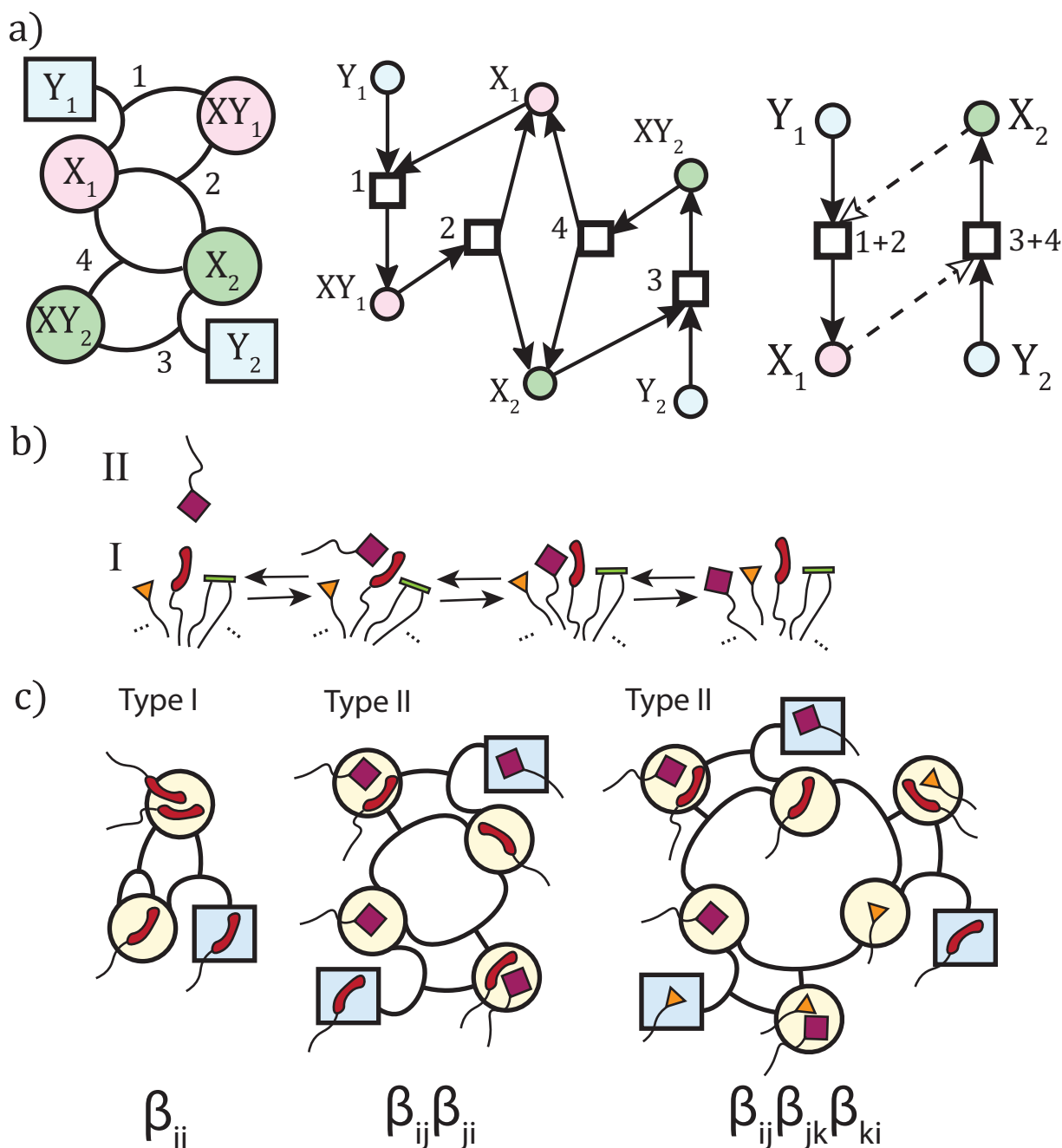


Figure S6: a. A type-II autocatalytic network with its feedstock compounds (or *Food set*), as encountered in GARD. Colored nodes highlight two distinct allocatalytic cycles that yield an autocatalytic cycle when combined. b. The same network, in a bipartite graph representation used in the RAF sets formalism. Specifying the mechanism in terms of uncatalyzed reaction steps removes the RAF property. c. A coarse-grained representation, where allocatalysts in the same allocatalytic cycle are represented by a single species, and each allocatalytic cycle has been replaced with a dashed line, to indicate the net reaction being catalyzed. b. A catalytic incorporation mechanism: the red (telephone shape) amphiphile forms a complex with the purple (square shape) amphiphile, which mediates its incorporation in a micelle or vesicle. c. Autocatalytic networks of co-assembling amphiphiles. Amphiphiles in square nodes are reservoir species, those in circular nodes represent amphiphiles in a micelle or membrane. Diagonal terms of the catalytic matrix encode type I autocatalysis, i.e. direct self-incorporation. All other autocatalysis (cross-incorporation) is of type II: sequences of nonoverlapping allocatalytic cycles.

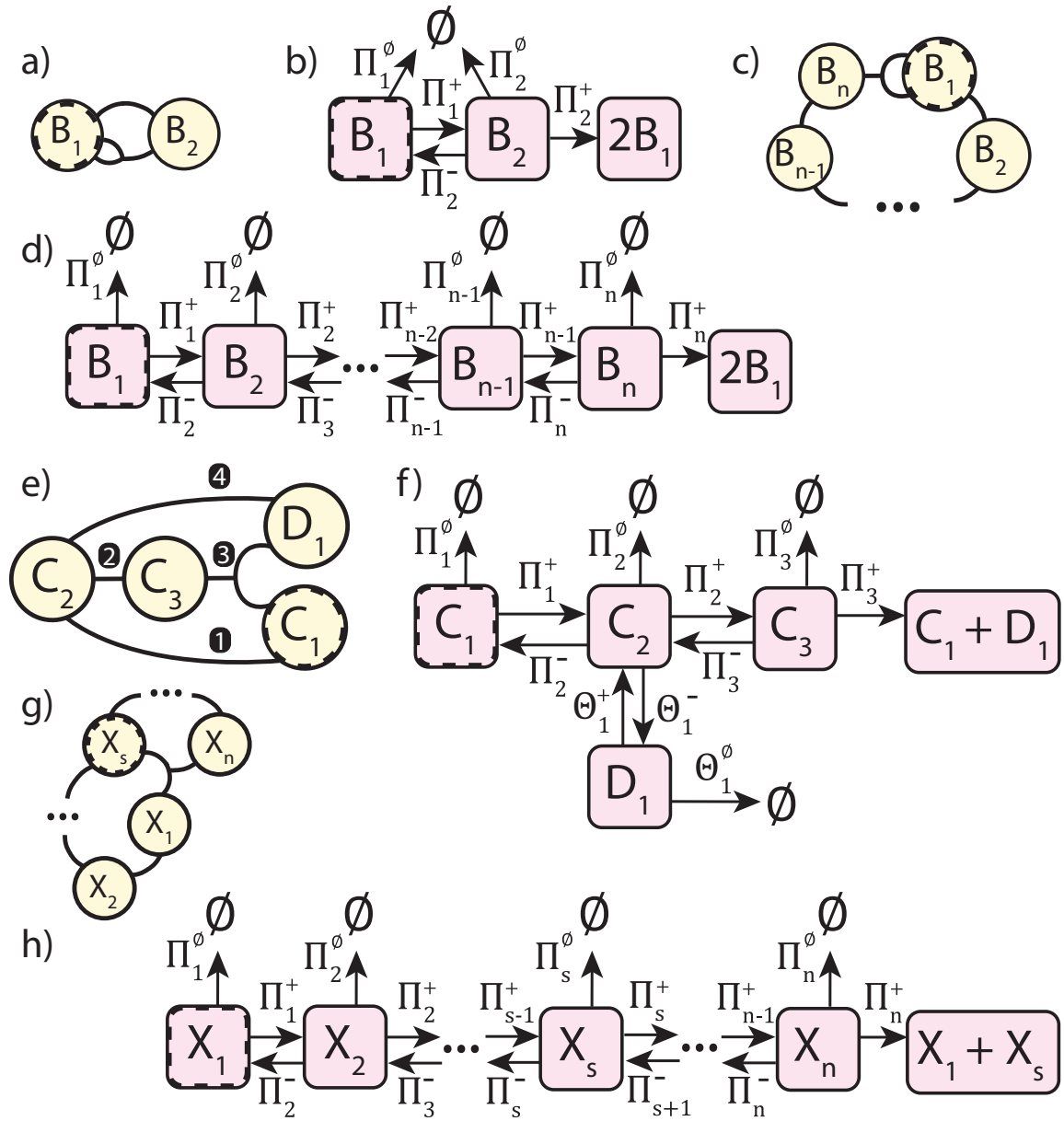


Figure S7: a. A type-I subnetwork. B_1 and B_2 reversibly interconvert, B_2 can also irreversibly form two B_1 , marked by the forked edge. b. State graph, Π_k^+ denotes the probability that, starting at B_k , the next transition will be a step forward in the cycle, Π_k^- a step backward, and Π_k^\emptyset a degradation. Fragmentation (yielding $2B_1$) and degradation (\emptyset) are absorbing states, attained with probabilities p_c and $1 - p_c$ respectively. c. Autocatalytic core for a type-I cycle with n nodes. d. State graph for c. e. schematic for an autocatalytic core for a type III cycle. f. State graph for e. g. general schematic for an autocatalytic core for a type II cycle with a single fragmentation step. h. State graph for g.

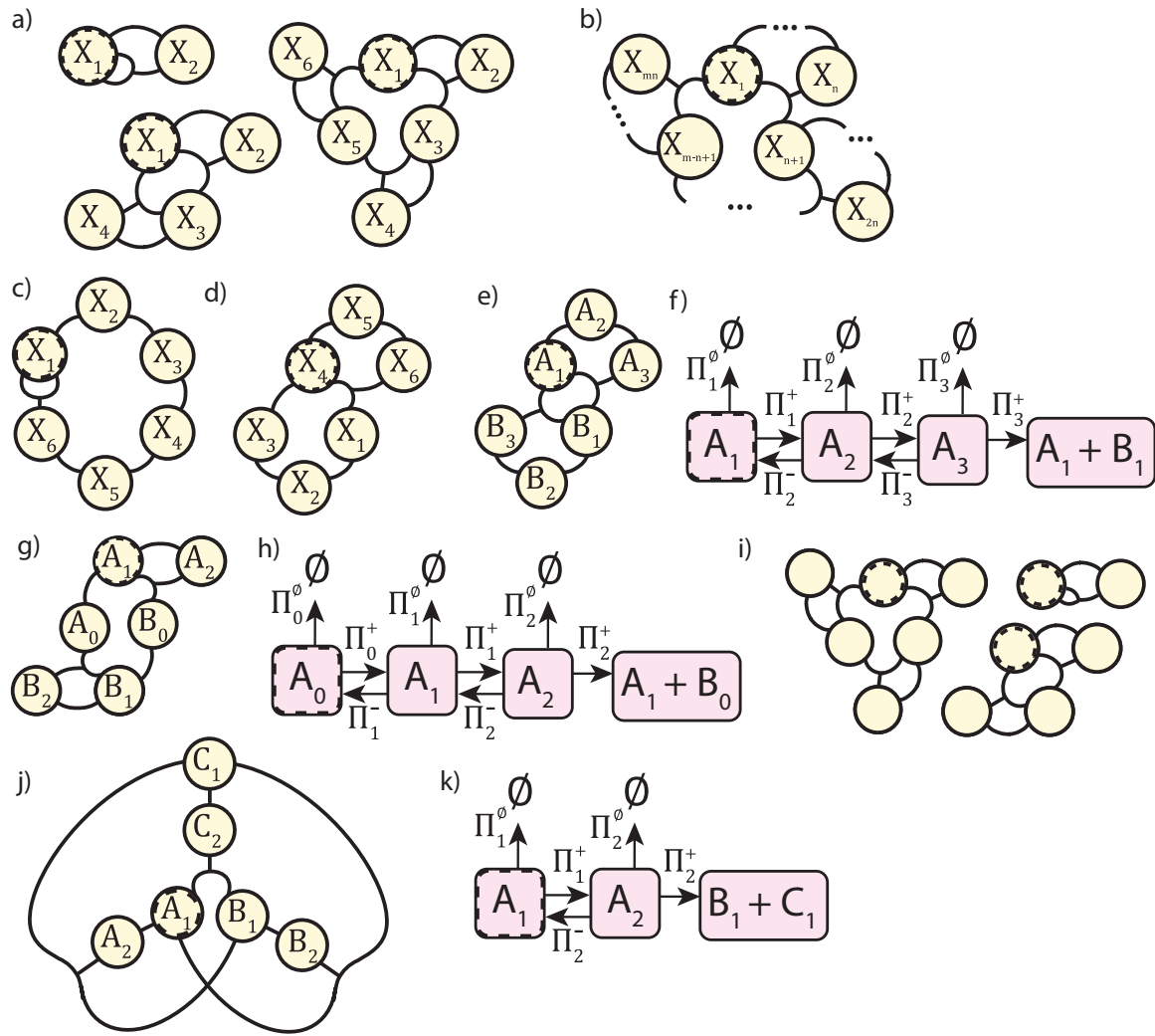


Figure S8: a) three motifs with the same $P_{ex}(A_k)$, when the transition network follows the same symmetry as the network structure. b) A more general case: a multiple of allocatalytic cycles of size n . c) 6-membered type I cycle. d) a 6-membered type II cycle. e) a 6-membered type III cycle. f) transition network for one of the two allocatalytic cycles. g) a 6-membered type III cycle. The transition of a precursor to allocatalyst is not mediated by an allocatalytic cycle, and hence this is not a RAF. h) Transition network. i) a trio of symmetric analogues. j) a type V autocatalytic core. k) transition network for j).

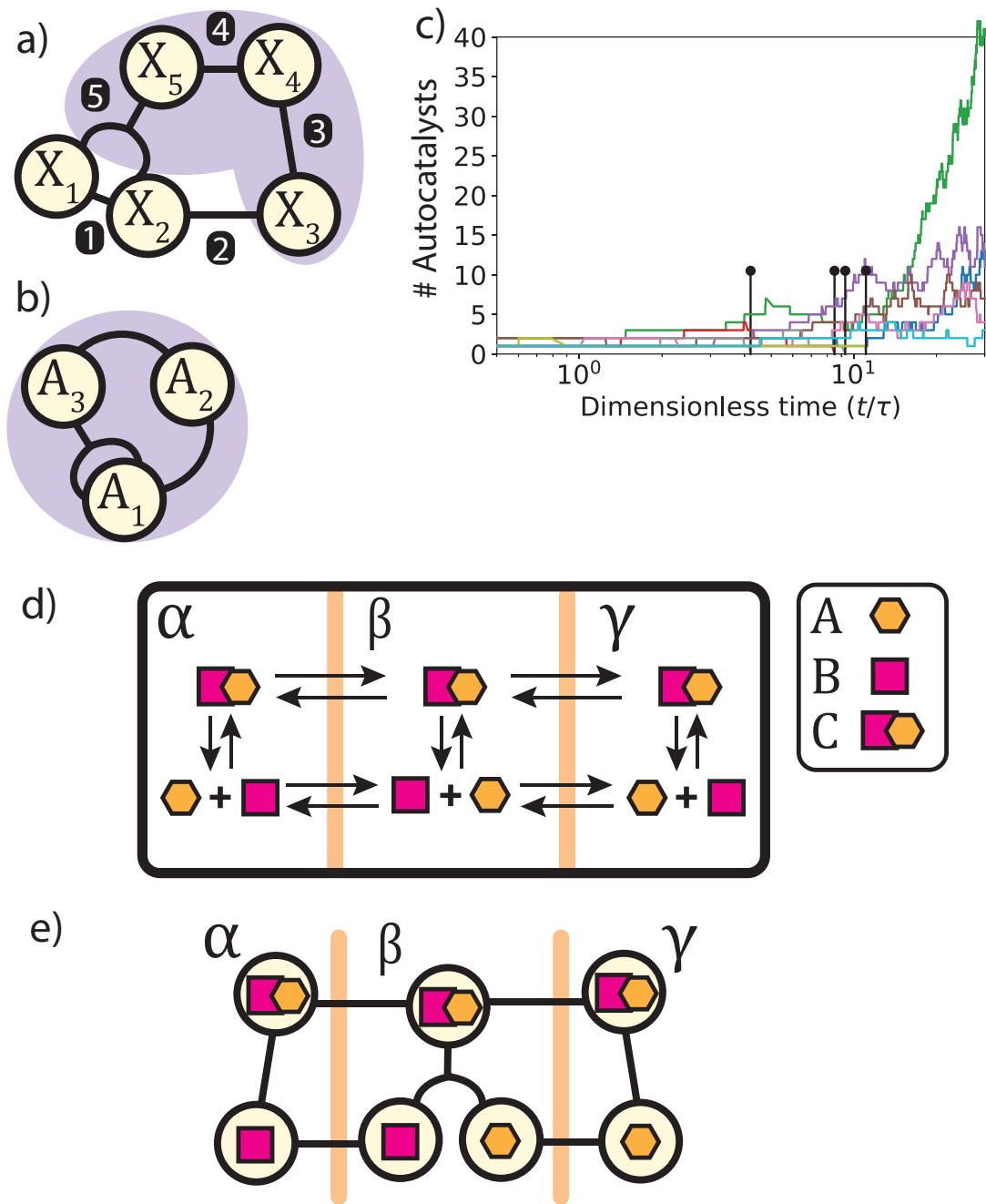


Figure S9: a) description in terms of X_k . Only the species in the purple circle undergo irreversible transitions towards absorbing states: degradation of X_3 (r6) and X_4 (r7), fragmentation of X_5 (r5). b) An effective network with the same statistics for P_{ex} as a), obtained by removing X_1 and X_2 . c) Simulation using Gillespie's Algorithm. Extinction events are marked with black pin. d) three-compartment network with a single bimolecular chemical reaction. e) autocatalytic core. The use of three compartment allows to construct the reactions to complete the cycle (the ears) directly from the reproduction step.